

Review

Metal Organic Frameworks as Heterogeneous Catalysts in Olefin Epoxidation and Carbon Dioxide Cycloaddition

Alessia Tombesi ¹ and Claudio Pettinari ^{2,*} 

¹ Chemistry Section, School of Science and Technology, University of Camerino, Via S. Agostino 1, 62032 Camerino, Italy; alessia.tombesi@unicam.it

² Chemistry Section, School of Pharmacy, University of Camerino, Via S. Agostino 1, 62032 Camerino, Italy

* Correspondence: claudio.pettinari@unicam.it

Abstract: Metal–organic frameworks (MOFs) are a family of porous crystalline materials that serve in some cases as versatile platforms for catalysis. In this review, we overview the recent developments about the use of these species as heterogeneous catalysts in olefin epoxidation and carbon dioxide cycloaddition. We report the most important results obtained in this field relating them to the presence of specific organic linkers, metal nodes or clusters and mixed-metal species. Recent advances obtained with MOF nanocomposites were also described. Finally we compare the results and summarize the major insights in specific Tables, outlining the major challenges for this emerging field. This work could promote new research aimed at producing coordination polymers and MOFs able to catalyse a broader range of CO₂ consuming reactions.

Keywords: heterogenous catalyst; metal–organic framework (MOF); olefin epoxidation; carbon dioxide cycloaddition



Citation: Tombesi, A.; Pettinari, C. Metal Organic Frameworks as Heterogeneous Catalysts in Olefin Epoxidation and Carbon Dioxide Cycloaddition. *Inorganics* **2021**, *9*, 81. <https://doi.org/10.3390/inorganics9110081>

Academic Editor: Duncan H. Gregory

Received: 28 September 2021

Accepted: 9 November 2021

Published: 15 November 2021

Publisher's Note: MDPI stays neutral with regard to jurisdictional claims in published maps and institutional affiliations.



Copyright: © 2021 by the authors. Licensee MDPI, Basel, Switzerland. This article is an open access article distributed under the terms and conditions of the Creative Commons Attribution (CC BY) license (<https://creativecommons.org/licenses/by/4.0/>).

1. Introduction

International Union of Pure and Applied Chemistry (IUPAC) defines MOFs as a coordination network with an open framework containing potential voids [1]. This emerging class of porous coordination polymers are formed by metal ion or cluster nodes and functional organic ligands, all connected through coordination bonds to form 1D, 2D or 3D networks (Figure 1) [2–6]. MOFs can be easily obtained by several different synthetic methods, such as electrochemical [7], solvothermal [8] and mechanochemical [9], slow diffusion [10], and more recently also by microwave-assisted heating [11].

The crystal structures of MOFs can be customized depending on the metal and ligand choice as also on the solvents and reaction conditions employed. [12] Due to the high surface areas [13] and ultrahigh porosity they are attractive for CH₄, CO₂, and H₂ sorption and storage. Most MOFs have higher volumetric H₂ and CH₄ storage capacities concerning traditional porous materials.

In recent years nanoscale MOFs have been also investigated for their potential applications in biomedicine, for example for drug delivery [14] and biological imaging [15], mainly for the possibility to use biocompatible building blocks. MOFs were employed as electrode materials for supercapacitors using Co-based coordination polymers [16], for magnetic and electronic devices [17], for water harvesting where H₂O is extracted from the air by solar energy [18], and finally also for non-linear optics [19].

The use of MOFs as a catalyst has been widely explored and several applications have been developed, for example in the production of fine chemicals [20], or the definition of possible new green protocols replacing non-eco-friendly catalysts [21]. Differences in activity and selectivity toward specific organic reactions are significantly dependent on the MOFs structure [22]. The main MOFs advantage, when we consider their use in catalysis, is in the possibility to design and predict the structural properties based on of linker features, coordination number and geometry of the metal.

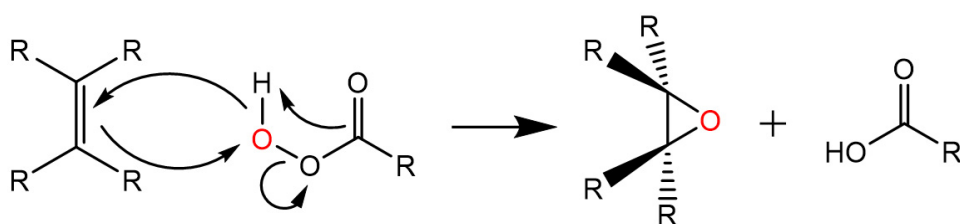


Figure 2. General mechanism of epoxidation of alkenes with peroxycarboxylic acid as co-catalyst.

CO₂ is the primary greenhouse gas in the atmosphere, and it is the cause of environmental and energy-related problems in the world. Nowadays, the development of new methods is fundamental to capture and convert CO₂ into useful chemical products to improve the environment and promote sustainable development. Several studies have been carried out on MOF's efficiency to capture CO₂. The linkers that connect the MOFs metal nodes are the major sites for CO₂ binding, and they can be chemically modified with functional groups to increase their interaction with CO₂. Moreover, unsaturated metals can be introduced in the MOFs structure. A significantly benefit generated from the possibility to have adequate quantities of CO₂ in concentrated form within a MOF is the possible use of CO₂ as a chemical reagent (Figure 3).

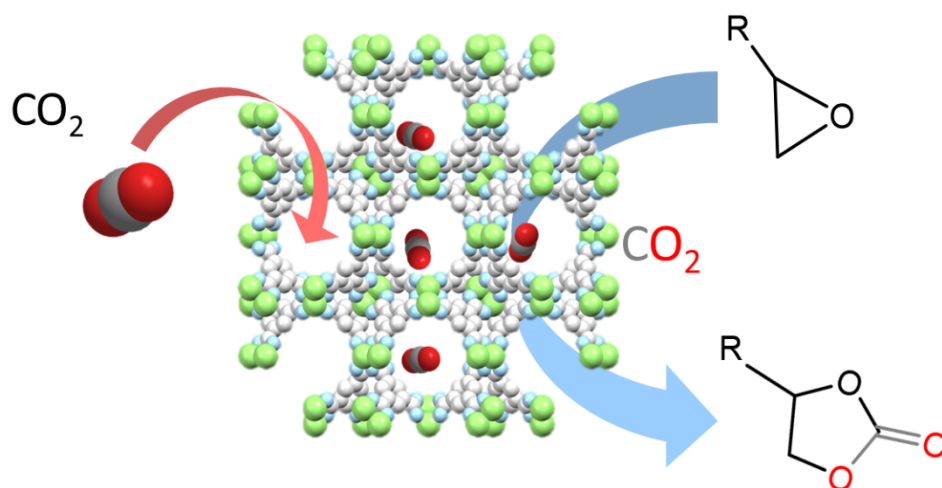


Figure 3. Representation of cycloaddition reaction of CO₂, captured by MOFs, to epoxides.

A significant number of MOFs has been recently reported to catalyse the CO₂ cycloaddition reaction to epoxides to give cyclic organic carbonates (OCs) and several papers describe the potential and effectiveness of MOFs in this important process, so it is necessary to identify better strategies to build new advanced materials as MOFs or MOF-based species to grow selectivity, capacity, and conversion of this catalytic reaction.

2. Olefin Epoxidation

C=C bond epoxidation is an attractive reaction for industrial process to obtain raw materials for epoxy resin, polymers, and pharmaceutical intermediates. Although homogenous catalysts in the epoxidation of alkene have been largely studied in the past few decades, the separation from the reaction mixture and its subsequent reusability remain open challenges [26,27].

Very recently, taking advantage of the tunability of MOFs, several transition metal-based epoxidation catalysts have been developed using MOFs synthesis in combination with post-synthetic modification. Several literature reports require utilization of expensive transition metals, but in the last period also metals like Cu, a classic non-noble transition metal, abundant, inexpensive, and non-toxic, become appealing catalyst sources.

2.1. Metal Nodes/Clusters as Catalytically Active Sites

MOFs can be applied as ideal platforms for heterogeneous catalysis towards olefin epoxidation thanks to several structural features with intrinsic catalytic activity such as the coordinatively unsaturated sites on MOFs nodes, defects, and catalytically active organic linkers.

Three pillared-layered Co₆-MOFs were utilized as heterogeneous catalysts for the selective oxidation of styrene using air, and benzyl alcohol with oxygen. The hexaprismatic [Co₆(μ₃-OH)₆] cluster with different variable valences activate the oxygen molecule for aerobic epoxidation of alkenes [28]. In Co₆-MOF-3, large pores facilitated the mass transfer giving the fastest reaction rate with high conversion and good selectivity for oxidation of both styrene and benzyl alcohol [29].

The 2D-cobalt (II)-based coordination polymer, $\{(Co(L2)H_2O)_2 \cdot H_2O\}_n$, have been obtained by hydrothermal synthesis using the histidine derivative 4-((1-carboxy-2-(1H-imidazol-4-yl)ethylamino)methyl)benzoic acid (H₂L2) as ligand. It has been investigated as heterogeneous catalysts on the allylic oxidation of cyclohexene (Appendix A).

The presence of a Co(II) open site on the surface maximizes the catalytic productivity, giving 82.56% of conversion and 71% of *tert*-butyl-2-cyclohexenyl-1-peroxide. Moreover, a Co(II)-based catalyst exhibits similar activity over five cycles without metal leaching [30] (Table 1).

The static and rotary hydrothermally synthetic method could affect significantly both the process of crystallization and heterogeneous catalytic activity of MOFs in the epoxidation reaction. For example, Co-MOF-150-2, hydrothermally synthesized by rotary crystallization at 150 rpm for 2 h, has reached 95.7% yield of 2,3-epoxypinane from α -pinene in aerobic conditions. The high catalytic activity of Co-MOF-150-2 is due to the better exposure of the metal active in the high crystalline structure, where the lamellar layer was more homogenous. The thinner Co-MOF-150-2 was also investigated in the epoxidation of the other olefins. Additionally, the catalytic activity was relevant for cyclic olefins like cyclooctene (78.5% of conversion after 5h of reaction) and for linear olefins (after 12 h 87.2% of 1-decene was transformed into the epoxide) [31].

A Co-MOF has been prepared under surfactant-thermal condition: NTUZ30 has been obtained with two different secondary building units (SBU), i.e., the unusual trinuclear [Co₃(μ₃-OH)(COO)₇] and [Co(COO)₄]. The cobalt sites onto the surface can convert *trans*-stilbene into the corresponding epoxide with excellent selectivity and high conversion [32].

A new 8-connected cobalt network (NH₄)₂[Co₃(Ina)(BDC)₃(HCOO)] has been generated from dicarboxylate (BDC = 1,4-benzenedicarboxylate) and pillar isonicotinate (Ina = isonicotinate) ligands with unusual Co₃ paddle-wheel cluster. The high number of unsaturated Co active sites available and the regular crystalline structure gave a great catalytic performance for cyclooctene epoxidation with a satisfactory TOF (turnover frequency) of 1370 [33].

Cu-containing MOFs look like promising catalysts for selective oxidation reactions. Generally, the selective oxidation of alkene goes through a radical reaction pathway in which molecular oxygen, or an oxidizing agent is present. Upon coordination of the oxidizing agent to Cu(II) (Figure 4), peroxy radicals are formed which then react with olefin to form the oxidized products [34,35].

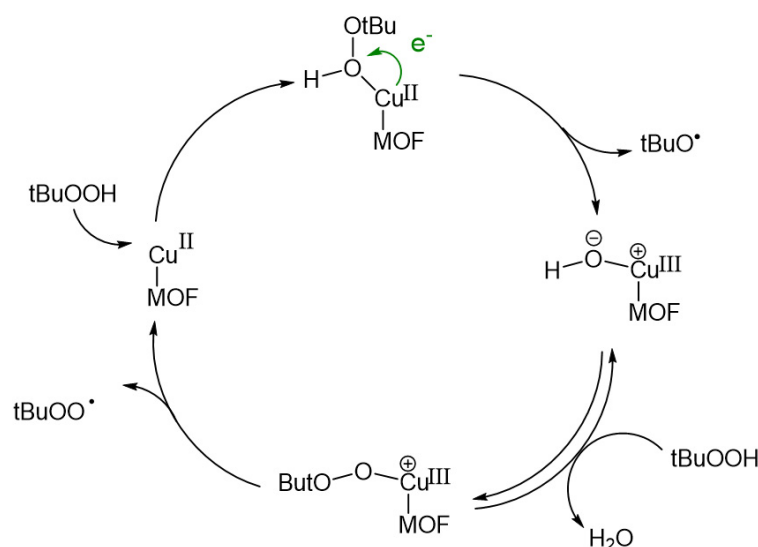


Figure 4. Schematic representation of the formation of *tert*-butylperoxyl ($t\text{BuOO}\cdot$) and *tert*-butoxyl radicals ($t\text{BuO}\cdot$) catalyzed by the Cu(II) sites of MOF.

By using $\text{Cu}_4\text{O}(\text{OH})_2(\text{Me}_2\text{trz-pba})_4$ ($\text{Me}_2\text{trz-pba}$ = 4-(3,5-dimethyl-4-*H*-1,2,4-triazol-4-yl)benzoate) and $\text{Cu}(\text{Me-4py-trz-ia})$ (Me-4py-trz-ia = 5-(3methyl-5-(pyridine-4-yl)4*H*-1,2,4-triazol-4-yl)isophthalate) a significantly higher catalytic activity in the epoxidation of cyclooctane with respect to $\text{Cu}_3(\text{BTC})_2$ (HKUST-1) has been found, due to the different coordination environment at the catalytically active Cu sites [36]. The catalytic performances of Cu-MOF nanosheets for cyclooctene and 1-hexene epoxidation were nearly twice higher than that of bulk $\text{Cu}_3(\text{BDC})_2$ crystals. This behaviour is attributed to the better exposure of a greater number of active sites on the surface of the Cu(BDC) nanosheets, which become more available during the reaction. The synthetic procedure must regulate the nanosheet thickness by controlling the dissolution rate of Cu^{2+} from $\text{Cu}(\text{OH})_2$ precursor and tuning the solvent composition. Moreover, the epoxide yield, after 5 cycles with CuMOF nanosheets, remains 96% [37] (Table 1).

In $\text{Cu}_4\text{O}(\text{OH})_2(\text{Me}_2\text{trz-pba})_4$, the $\text{Cu}_4(\mu_4\text{-O})(\mu_2\text{-OH})$ tetrahedral node possesses two Cu^{2+} ions bridged by hydroxyl group, which take part in the activation of oxidating agent TBHP, promoting a quicker formation of *tert*-butoxyl and *tert*-butylperoxyl radicals, whereas in $\text{Cu}(\text{Me-4py-trz-ia})$ the asymmetric unit contains two crystallographically independent Cu^{2+} ions. One of them possesses two unsaturated sites that could cause a change in Lewis acidity and generate different redox properties [36].

Oxidation of nonterminal olefin, such as *cis*-stilbene and cyclooctene, occurs with 94% and 98% conversion, when the activated $\{[\text{Cu}(\text{L3-H})(\text{DMA})]\cdot\text{DMA}\cdot 2\text{H}_2\text{O}\}_\infty$ MOF ($\text{H}_3\text{L3}$ = tris(4'-carboxybiphenyl)amine; DMA = *N,N*-dimethylacetamide) was used. The activation was carried out at 200° C for 8 h under vacuum to remove DMA coordinated molecules and produce unsaturated Cu sites that act as Lewis acid [38].

Nbo-type Cu-MOFs, synthesized from the meta-substituted ligand 2,2',6,6'-tetramethoxy-4,4'-biphenyldicarboxylic acid ($\text{H}_2\text{L4}$) and copper nitrate $[\text{Cu}_3(\text{L4})_3(\text{H}_2\text{O})_2(\text{DMF})]_n$, possess a high density of catalytic sites in optimal position within the channels, in which oxidation of nonterminal olefins (e.g., norbornene, *trans*- β -methylstyrene, *cis*- β -methylstyrene, and *trans*-stilbene) occurs with 99% conversion and 99% selectivity [39]. Moreover, the less reactive aliphatic alkenes such as 1-octene and *trans*-4-octene showed moderate conversions with good selectivity.

Epoxidation of cyclohexene achieves the 100% of conversion in presence of H_2O_2 after 8h when 2D metal carboxylate framework $\{2(\text{Him})\cdot[\text{Cu}(\text{pdc})_2]\}_n$ has been involved as a heterogeneous catalyst. $\{2(\text{Him})\cdot[\text{Cu}(\text{pdc})_2]\}_n$ (H_2pdc = pyridine-2,5-dicarboxylic acid, Him = imidazole) was obtained through structural inter-conversions starting from $[\text{Mg}(\text{H}_2\text{O})_6][\text{Cu}(\text{pdc})_2]\cdot 2\text{H}_2\text{O}$ increasing the imidazole concentration by hydrothermal

treatment. The structure of $\{2(\text{Him})\cdot[\text{Cu}(\text{pdc})_2]\}_n$ derives from the connection of $\{[\text{Cu}(\text{pdc})_2]\}_n$ ribbon-like 1D chains by intermolecular H-bonding between hydrogen in the imidazolium ion and the free carboxylate oxygens of pdc^{2-} , this 2D supramolecular structure being crucial to ensure the reaction heterogeneity. Likewise, 1-hexene showed almost complete conversion but increasing the chain length of alkene, the double bond becomes sterically hindered limiting the approach to the active site, and the catalytic activity decreases [40] (Table 1).

High stable zirconium-based MOFs are largely used as active and recyclable catalysts for a variety of catalytic transformations. The catalytic activity of UiO-66 and other Zr-MOFs can be greatly attributed to the presence of random defects in their crystalline structure [41–43]. These accessible Lewis acid centers, sometimes in conjunction with Lewis basic sites (e.g., amine groups) in functionalized linker, lead to a significant increase in the catalytic activity [44,45].

Recently, the reaction mechanism underlying both thioether oxidation in nonprotic solvents and epoxidation of electron-deficient C=C bonds in α,β -unsaturated ketones, catalysed by UiO-66 and UiO-67 has been exhaustively investigated [46]. This study suggests the formation of hydroperoxo zirconium species as an oxidant. As already known, the oxidation of less-reactive α,β -unsaturated carbonyl compounds was accompanied by oxidation of MeCN solvent and H_2O_2 under basic conditions [47], but this nucleophilic peroxy species derived from H_2O_2 and Zr-MOF can contribute to the epoxidation of the electron-deficient C=C bonds because the reaction readily proceeds even in ethyl acetate.

Table 1. MOFs with metal Nodes/clusters active in olefin epoxidation.

MOF	Substrate	Reaction Data T (°C) P (atm) Time (h)			Oxidant/Cocatalyst/ Solvent ^a	Conversion %	Epoxide Selectivity%	Ref.
Co6-MOF-3	Styrene	100	1	14	Air/-/DMF	99	90	[29]
Co-MOF-150-2	α -Pinene	90	1	5	Air/CHP/-	99.5	96.2	[31]
	Cyclooctene	90	1	5	Air/CHP/-	78.5	-	[31]
	1-Decene	90	1	5	Air/CHP/-	87.2	-	[31]
NTUZ30	<i>trans</i> -Stilbene	100	7	1	O_2 /-/-	98.2	95.6	[32]
$(\text{NH}_4)_2[\text{Co}_3(\text{Ina})(\text{BDC})_3(\text{HCOO})]$	Cyclooctene	35	1.5	1	IBA/-/CH ₃ CN	98	92	[33]
$\text{Cu}_3(\text{BTC})_2$	Cyclooctene	75	1	24	Air/TBHP/Toluene	20	-	[36]
	1-Hexene	25	1		Air/TBHP/Toluene	30.5	-	[36]
Cu-MOF nanosheets	Cyclooctene	25	1	12	O_2 /-/CH ₃ CN	100	-	[37]
	1-Hexene	25	1		O_2 /-/CH ₃ CN	67.2	-	[37]
$\text{Cu}_4\text{O}(\text{OH})_2(\text{Me}_2\text{trz-pba})_4$	Cyclooctene	75	1	24	Air/TBHP/Toluene	90	80	[36]
$\text{Cu}(\text{Me-4py-trz-ia})$	Cyclooctene	75	1	24	Air/TBHP/Toluene	38	60	[36]
$\{[\text{Cu}(\text{L3-H})(\text{DMA})]\cdot\text{DMA}\cdot 2\text{H}_2\text{O}\}_\infty$	<i>cis</i> -Stilbene	60	1	24	<i>t</i> -BuOOH/-/CH ₃ CN	94.4	-	[38]
	Cyclooctene	60	1	24	<i>t</i> -BuOOH/-/CH ₃ CN	98	-	[38]
$\{2(\text{Him})\cdot[\text{Cu}(\text{pdc})_2]\}_n$	Cyclohexene	60	1	8	Air/ H_2O_2 /EtOH	100	-	[38]
	Cyclooctene	60	1	8	Air/ H_2O_2 /EtOH	100	-	[38]
$[\text{Cu}_3(\text{L4})_3(\text{H}_2\text{O})_2(\text{DMF})]_n$	Styrene	40	1	6	O_2 /TMA/CH ₃ CN	90	88	[39]
	Cyclooctene	40	1	6	O_2 /TMA/CH ₃ CN	99	99	[39]
$\{(\text{Co}(\text{L2})(\text{H}_2\text{O}))_2\cdot\text{H}_2\text{O}\}_n$	Cyclohexene	60	1	6	<i>t</i> -BuOOH/-/-	82.56	71.93	[30]
UiO-66	2-Cyclohexen-1-one	70	1	1	H_2O_2 /-/CH ₃ CN	20	60	[46]
	2-Cyclohexen-1-one	70	1	2	H_2O_2 /-/EtOAc	18	45	[46]
	Chalcone	70	1	0.5	H_2O_2 /-/EtOAc	30	50	[46]
UiO-67	2-Cyclohexen-1-one	70	1	1	H_2O_2 /-/CH ₃ CN	20	55	[46]
	2-Cyclohexen-1-one	70	1	2	H_2O_2 /-/EtOAc	20	55	[46]
	Chalcone	70	1	0.5	H_2O_2 /-/CH ₃ CN	40	40	[46]

^a *t*BuOOH = *tert*-butyl hydroperoxide; CHP = cumene hydroperoxide; TBHP = *tert*-butylhydroperoxide; IBA = isobutyraldehyde; TMA = trimethylacetaldehyde.

2.2. Mixed-Metal Species

Many efforts have been made to improve the catalytic performance of MOFs, and one possible way is the construction of bimetallic clusters by functionalization of metal nodes/clusters with active transition metals to afford MOF-based catalysts with high performance.

A hydrothermal reaction has been used to synthesise $\text{Cu}_x\text{-Co}_y\text{-MOF}$, where $\text{Co}(\text{NO}_3)_2 \cdot 6\text{H}_2\text{O}$ and $\text{Cu}(\text{NO}_3)_2 \cdot 3\text{H}_2\text{O}$ inorganic metal salts have been one-pot added to a ligand solution in different molar ratios. In addition to the high catalytic activity by doping Cu-MOF with Co, a better selectivity to produce styrene oxide is achieved. At the optimal reaction conditions, the conversion and the selectivity of styrene to styrene oxide increased to 97.81% and 83.04%, respectively, by using $\text{Cu}_{0.25}\text{-Co}_{0.75}\text{-MOF}$, the catalyst of this series with higher content of Co^{2+} [48]. Another study showed how the conversion of styrene-to-styrene oxide increased rapidly when Mn ions were introduced into a Cu-MOF with the two ligands 2,5-dihydroxyterephthalic acid (H_4DHTA) and 2-picolinic acid (PCA). $\text{Mn}_{0.1}\text{Cu}_{0.9}\text{-MOF}$ exhibits interesting catalytic activity for the epoxidations of various aromatic and cyclic olefins and a weak activity on decomposition of H_2O_2 . Styrene can be oxidized by H_2O_2 , through peroxyb carbonate-assisted catalysis, the styrene oxide yield achieving 85% in the presence of $\text{Mn}_{0.1}\text{Cu}_{0.9}\text{-MOF}$ at 0 °C for 6 h [49].

To increase conversion and selectivity in the solvent-free aerobic oxidation of olefins, MOF catalysts based on *3d* metal copper (II), cobalt (II) and H_2ODA (oxydiacetic acid) containing lanthanum (III) as *4f* ions $\{[\text{La}_2\text{Cu}_3(\mu\text{-H}_2\text{O})(\text{ODA})_6(\text{H}_2\text{O})_3] \cdot 3\text{H}_2\text{O}\}_n$ (LaCuODA) and $\{[\text{La}_2\text{Co}_3(\text{ODA})_6(\text{H}_2\text{O})_6] \cdot 12\text{H}_2\text{O}\}_n$ (LaCoODA) were employed. Catalytic studies pointed out the difference in aerobic oxidation of cyclohexene performances due to different physicochemical properties, surface area and redox properties of the metals (Table 2). [50] LaCoODA , based on Co(II), showed better conversion and selectivity for 2-cyclohexen-1-one. This is due to the structural differences between the square planar LaCuODA and the octahedral LaCoODA , in the latter case the water molecules could easily leave the channels to foster interaction between the active sites and the oxidant/catalyst. Moreover, the acid properties of the copper(II) ions are less effective than the redox properties of cobalt(II) ones, as far as the catalytic performances [34,51].

In NU-1000 single-ion-based iron(III) species have been incorporated using solution-phase post-synthetic metalation with two different iron(III) precursors. The resulting NU-1000-Fe- NO_3 and NU-1000-Fe-Cl frameworks show two crystallographically independent Fe sites (Fe1 resides in the c-pore and Fe2 in the hexagonal mesopore), coordinated to the bridging and terminal oxygens of the Zr6 node, with Fe–O distances in NU-1000-Fe-Cl being much longer than those of NU-1000-Fe- NO_3 (Figure 5) [52]. Epoxidation of cyclohexene in vapour H_2O_2 with NU-1000-Fe- NO_3 as catalysts initially yields cyclohexene epoxide derived from heterolytic activation of H_2O_2 , which in turn hydrolyzes rapidly to *trans*-cyclohexanediol. Otherwise, NU-1000-Fe-Cl yields a mixture of products and by-products, derived from the radical oxidation products due to homolytic activation of H_2O_2 [53,54]. This behaviour is probably due to the difference in the metal–node distance between the frameworks, the active site rearranging differently.

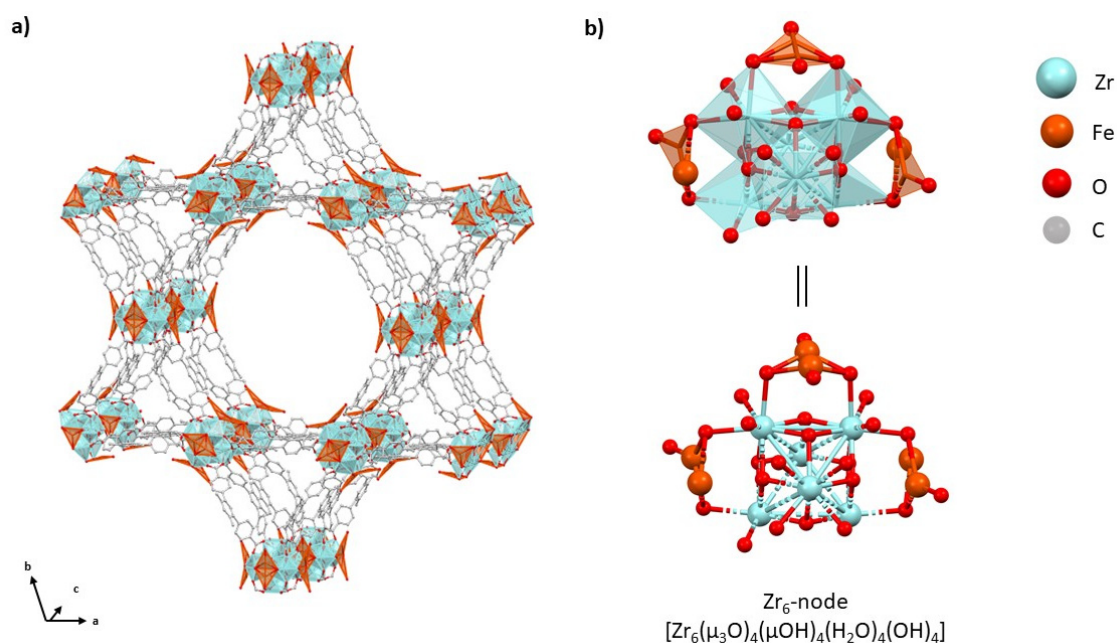


Figure 5. (a) Crystal structures of NU-1000-Fe-NO₃ (b) Structures of the inorganic Zr₆-nodes.

One-step template-free synthesis of ultrathin (~5 nm) mixed-valence {V16} clusters-based MOF nanosheets [Ni(4,4'-bpy)₂]₂ [V^{IV}V^VO₃₈Cl]·(4,4'-bpy)·6H₂O (NENU-MV-1) has been also reported. A large number of vanadium catalytically active sites in the NENU-MV-1 nanosheet allowed excellent cyclohexene oxidation under air exhibiting a conversion of 95%. Moreover, the nanometer scale of the catalyst increased the catalytic activity 2.7 times compared to the bulk crystal (0.25 mm) for olefin epoxidation. Excellent catalytic performances have been shown for different olefin substrates [55].

Table 2. Mixed Metal MOFs in Olefin Epoxidation.

MOF	Substrate	Reaction Data			Oxidant/Cocatalyst/Solvent ^a	Conversion %	Epoxide Selectivity%	Ref.
		T (°C)	P (atm)	Time (h)				
Mn _{0.1} Cu _{0.9} -MOF	Styrene	0	1	6	H ₂ O ₂ /-/DMF	90.2	94.3	[49]
Cu _{0.25} -Co _{0.75} -MOF	Styrene	80	1	8	Air/TBHP/t-BuOH/H ₂ O ₂	97.81	83.4	[48]
Zn1Co1-ZIF	Styrene	100	1	24	TBHP/-/DMF	99	71.31	[56]
LaCoODA	Cyclohexene	75	1	24	O ₂ flow/-/-	85	75	[50]
LaCuODA	Cyclohexene	75	1	24	O ₂ flow/-/-	67	55	[50]
NENU-MV-1	Cyclohexene	35	1	4	Air/IBA/CH ₃ CN	95	86	[55]
NU-1000-Fe-Cl	Cyclohexene	120	0.03	3	H ₂ O ₂ /-/	-	70	[52]
NU-1000-Fe-Cl	Cyclohexene	120	0.03	3	H ₂ O ₂ /-/	-	70	[52]

^a tBuOH = *tert*-butyl alcohol; TBHP = *tert*-butylhydroperoxide; IBA = isobutyraldehyde.

2.3. Organic Linkers with Functional Catalytically Active Sites

Functional groups such as amino, pyridyl, amide, sulfonic acid, etc. present in organic linkers serve as active sites for catalysis and strongly influence the intrinsic catalytic activity of the MOFs through inductive effects. In addition, organic linkers can be catalytically active when organic functional groups and/or functional molecular catalysts (e.g., metalloporphyrins, salen and related ligands, chiral molecules, Schiff-base complexes, etc.) are introduced by post-synthetic ways. Alternatively, the same functional molecular catalysts can also be used as building units to fabricate MOFs.

Molybdenum complexes have been widely applied as homogeneous catalysts for the epoxidation of alkenes by H₂O₂ and organic hydroperoxide, a complete conversion and selectivity being reported. To overcome the recoverability and reusability issues correlated

to the use of homogeneous molybdenum catalysts, molybdenylacetylacetonate has been supported on TMU-16-NH₂ [Zn₂(NH₂-BDC)₂(4-bpdh)]·3DMF, an amine-functionalized two-fold interpenetrated MOF via dative and combined covalent and dative post-synthetic modification [57].

A high porous NU-1000 MOF has been post-modified with the chiral L-tartaric acid, by SALI (solvent-assisted ligand incorporation) to build a chiral Zr-based MOF [C-NU-1000] [58]. Moreover, another active catalytic site, molybdenyl acetylacetonate, MoO₂(acac)₂, was incorporated on chiral NU-1000 to explore catalytic performance in the asymmetric epoxidation of olefins (Figure 6a) [59]. When olefins approach by pro-S- or R-face to the catalytic active center, they interact with the OH group of the tartrate through H-bond which induces chirality generating two chiral intermediates. The [C-NU-1000-Mo] catalyst, used in the epoxidation of styrene and 1-decene, can discriminate the S configuration in epoxides (Figure 6b).

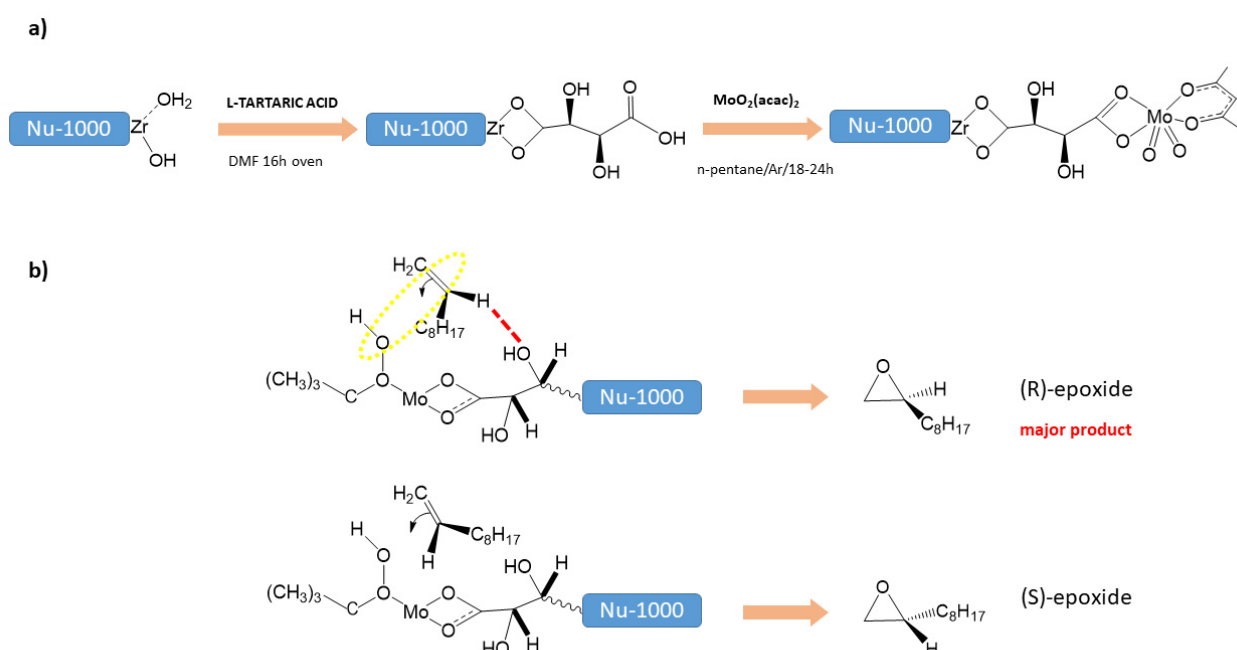


Figure 6. (a) The preparation of [C-NU-1000-Mo] catalyst with solvent-assisted ligand incorporation (SALI); (b) simplification of the chirality induction mechanism of [C-NU-1000-Mo] when olefins approach by pro-S- or R-face to the catalytic active center.

The free amine group available on UiO-66-NH₂ has been post-synthetically modified with salicylaldehyde (SA) or thiophene-2-carbaldehyde (TC) to graft a Schiff base in which MoO₂(acac)₂ could be immobilized. Efficient olefin epoxidation catalysed by UiO-66-NH₂-SA-Mo and UiO-66-NH₂-TC-Mo has been described and no Mo active site leaching was detected [60]. In the same way, MoO(O₂)₂·2DMF was immobilized onto UiO-66(NH₂) functionalized with salicylaldehyde (Sal) (UiO-66-sal-MoD), pyridine-2-aldehyde (PI) (UiO-66-PI-MoD) and 2-pyridine chloride (PC) (UiO-66-PC-MoD). All of them allowed a high dispersion of Mo catalyst, the large pores of MOFs guarantee adequate contact between the substrate and the catalytic active center, thus improving the efficiency of cyclic olefins epoxidation [61].

Molybdenum(VI) oxide was deposited on the eight-connected Zr₆(μ₃-O)₄(μ₃-OH)₄(H₂O)₄(OH)₄ nodes connected by 1,3,5,8-(*p*-benzoate) pyrene linkers (TBAPy⁴⁻) of the mesoporous NU-1000, via condensation phase through solvothermal deposition in MOF (SIM) [62]. The stable Mo-SIM system exhibits a high conversion for cyclohexene epoxidation without leaching of molybdenum catalyst compared to Mo supported on bulk zirconia (Mo-ZrO₂), in which significant leaching of the catalytic species has been observed [60].

Molybdenum tricarbonyl complexes are known to be effective catalysts for the epoxidation of olefins. They form an oxomolybdenum (VI) species in the presence of *tert*-butyl hydroperoxide (TBHP) as an oxidant which acts as highly active catalytic sites for the epoxidation of olefin. $M(CO)_6$ was deposited on UiO-66 and UiO-67 by chemical vapor deposition (CVD) treatment, UiO-66-Mo(CO)₃, and UiO-67-Mo(CO)₃ heterogeneous catalysts being fabricated. Herein, the larger tetrahedral and octahedral cavities of UiO-67 enable more accessibility of cyclooctene to catalytically active sites showing higher catalytic activity for the cyclooctene conversion than UiO-66-M(CO)₃ [33].

Several attempts have been made to immobilize oxovanadium(IV) complexes on different solid materials and create heterogeneous catalytic systems for the epoxidation of allylic alcohols [63–66]. A catalyst has been designed by immobilizing oxovanadium(IV) species on UiO-66(NH₂) via post-synthetic modification and by using two different pathways. At first, the amino-functionalized UiO-66(NH₂) was modified with salicylaldehyde to produce salicylideneimine modified UiO-66 (UiO-66-SI), subsequently [VO(acac)₂] was reacted with UiO-66-SI to give UiO-66-SI/VO(acac). In another pathway, UiO-66(NH₂) directly reacted with [VO(acac)₂] to produce UiO-66-N/VO(acac)₂ [67]. Excellent catalytic activity in the regioselective epoxidation of geraniol was obtained when UiO-66-SI/VO(acac) and UiO-66-N/VO(acac)₂ systems were employed by using reaction times of 60 and 120 min, respectively. The proper pore size of and the high dispersion of the catalytic sites on UiO-66-SI/VO(acac) and UiO-66-N/VO(acac)₂ guarantee good access of the substrate to the active sites.

Metallosalen-based crystalline porous materials have been realized for heterogeneous catalytic applications towards cyclopropanation, alkene epoxidation and hydrolytic kinetic resolution of epoxides with interesting enantioselectivities [5]. UiO-68-Me has been modified via post-synthetic exchange (PSE) with single- and mixed-M(salen) linker (M = Cu, Fe, Cr, V, Mn) to fabricate UiO-66(NH₂) attractive species for heterogeneous asymmetric catalysis, useful to overcome the problem of metal leaching. It was found that the single-M(salen) chiral MOFs (R)-UiO-68-Mn and (R)-UiO-68-Fe catalyse the epoxidation of alkenes to epoxides with up to a 98% ee of epoxide and 97% ee, respectively. The different catalytic metal centers in the mixed-(M)salen species UiO-68-Mn-Cr gave consecutive reactions starting from the epoxidation of alkene followed by ring-opening reaction of epoxide to produce the desired amino alcohol in 80–85% yields with 80–99.5% ee. Catalytic activity and enantioselectivity of all chiral UiO-68 catalysts remain unchanged for 10 cycles [68].

Encapsulation of Cu- or Ni-salen species in NH₂-MIL-101(Cr) through one-pot method gave a series of effective heterogeneous catalysts in the styrene oxidation under mild conditions. Specifically, the styrene conversion obtained using TBHP was 98.78%. The concentrated electronic density around Cu(II) in the Cu salen@NH₂-MIL-101(Cr) catalyst promoted the formation of tBuOOCu(III)-salen enhancing the selectivity to epoxide [69].

A recent synthetic strategy resides in the incorporation of different functionality in one single framework to generate a multivariate MOF (MTV-MOFs). On this basis, a chiral MOF based on multiple metallosalen bridging ligands has been synthesised. Firstly, M(salen)-derived dicarboxylate ligands H₂L^M [M = Cu, VO, CrCl, MnCl, Fe(OAc), and Co(OAc)] were synthesized by reactions of N,N'-bis(3-*tert*-butyl-5-(carboxyl)salicylide (H₄L₅) and the corresponding metal salts in MeOH at room temperature. Secondly, the crystals of binary or ternary MTV-MOFs (CuV, CuMn, CuCr, CuFe, and CuCo) were obtained by heating a 1:1 or 1:1:1 mixture of H₂L^M with Zn(NO₃)₂·6H₂O at 80 °C in DMF, [Zn₄O(L^{M,M'})₃] species is obtained. Both [Zn₄O(L^{5Cu,Mn})₃] and [Zn₄O(L^{5Cu,Fe})₃] showed efficient catalytic performances for asymmetric epoxidation of alkenes, affording up to 93% and 90% ee of the epoxides, respectively. Moreover, in the ternary heterogeneous catalyst [Zn₄O(L^{5Cu,Mn,Co})₃], the combination of Mn³⁺ and Co³⁺ promotes the epoxidation of alkene followed by enantioselective hydrolysis of epoxide to afford diols [70].

The achiral Zr-MOF, [PCN-224(Mn(Cl))], based on tetratopic ligand [manganese (chloride) tetrakis(4-carboxyphenyl)porphyrin [Mn(Cl)-TCPP], has been post-synthetically modified with tartrate anion, as a chiral auxiliary. The final chiral PCN-224-Mn(tart) contains

two active metal sites (Zr and Mn) as Lewis acid centers and the chiral tartrate counterion, as Brønsted acid sites (OH functional group) has been investigated as chiral nucleophile catalyst towards both asymmetric epoxidation and CO₂ fixation. Asymmetric epoxidation of several aromatic and aliphatic olefins like styrene, *trans*-stilbene, 4-methylstyrene, α -methylstyrene, 1-phenyl-1-cyclohexene, 1-decene, and 1-octene has been tested by using PCN-224-Mn(tart) with aldehyde as co-catalyst, CH₃CN, and O₂. The all-reaction conversions were completed with an optimum range of epoxide selectivity 83–100% and high ee (84–100%). Several factors allow high enantioselectivity in the formation of the epoxide: the framework porosity, the active Mn center, a preferred face of the olefin (pro-S or -R face) close to produce the more stable configuration, and the noncovalent interactions between H atom of the olefinic double bond of the preferred face and chiral centers (Table 3) [71].

Table 3. MOFs with functionalized organic linker in olefin epoxidation.

MOF	Substrate	Reaction Data			Oxidant/Cocatalyst/ Solvent ^a	Conversion %	Epoxide Selectivity%	Ref.
		T (°C)	P (atm)	Time (h)				
UiO-66-SI/VO(acac)	Geraniol	40	1	1	TBHP/-/CH ₂ Cl ₂	100	100	[67]
UiO-66-N/VO(acac) ₂	Geraniol	40	1	2	TBHP/-/CH ₂ Cl ₂	100	100	[67]
UiO-66-sal-MoD	<i>cis</i> -Cyclooctene	80	24	1	TBHP/-/CH ₃ CN	99	99	[61]
PCN-224-Mn(tart)	Styrene	60	1	4	O ₂ /IBA/CH ₃ CN	100	89	[71]
	<i>trans</i> -Stilbene	60	1	4	O ₂ /IBA/CH ₃ CN	80	100	[71]
	1-Phenyl-1-cyclohexene	60	1	4	O ₂ /IBA/CH ₃ CN	75	100	[71]
	1-Octene	60	1	4	O ₂ /IBA/CH ₃ CN	70	100	[71]
UiO-67-Mo(CO) ₃	Cyclooctene	55	3	1	TBHP/-/toluene	100	99	[33]
UiO-66-Mo(CO) ₃	Cyclooctene	55	3	1	TBHP/-/toluene	92	99	[33]
[C-NU-1000-Mo]	Styrene	120	0.03	5	H ₂ O ₂ /-/CH ₂ CH ₂ Cl ₂	100	86	[58]
	1-Octene	120	0.03	8	H ₂ O ₂ /-/CH ₂ CH ₂ Cl ₂	72	100	[58]
UiO-66-NH ₂ -SA-Mo	Cyclooctene	83	0.75	1	TBHP/-/CH ₂ CH ₂ Cl ₂	97	100	[60]
	Cyclohexene	83	1.5	1	TBHP/-/CH ₂ CH ₂ Cl ₂	93	100	[60]
	Styrene	83	5	1	TBHP/-/CH ₂ CH ₂ Cl ₂	87	92	[60]
	1-Octene	83	8	1	TBHP/-/CH ₂ CH ₂ Cl ₂	78	100	[60]
	1-Decene	83	10	1	TBHP/-/CH ₂ CH ₂ Cl ₂	79	100	[60]
UiO-66-NH ₂ -TC-Mo	Cyclooctene	83	1	1	TBHP/-/CH ₂ CH ₂ Cl ₂	94	100	[60]
	Cyclohexene	83	2	1	TBHP/-/CH ₂ CH ₂ Cl ₂	90	100	[60]
	Styrene	83	5	1	TBHP/-/CH ₂ CH ₂ Cl ₂	86	90	[60]
	1-Octene	83	8	1	TBHP/-/CH ₂ CH ₂ Cl ₂	75	100	[60]
	1-Decene	83	10.5	1	TBHP/-/CH ₂ CH ₂ Cl ₂	75	100	[60]
[Zn ₄ O(L ⁵ Cu,Fe) ₃]	2,2-Dimethyl-2 <i>H</i> -chromene	−20	1	36	MesPhIO/-/CHCl ₃	94	87 ee	[70]
[Zn ₄ O(L ⁵ Cu,Mn,Co) ₃]	3-Chloropropene	0	1	10	sPhIO/-/CHCl ₃	92	-	[70]
	Styrene	0	1	24	sPhIO/-/CH ₂ Cl ₂	63	-	[70]
UiO-66-PC-MoD	<i>cis</i> -Cyclooctene	80	24	1	TBHP/-/CH ₃ CN	90.7	99	[61]
Mo-SIM	Cyclohexene	60	1	7	TBHP/-/toluene	93	99	[59]
(R)-UiO-68-Mn	2,2-Dimethyl-2 <i>H</i> -chromene	0	1	10	sPhIO/-/CH ₂ Cl ₂	91	88 ee	[68]
UiO-66-PI-MoD	<i>cis</i> -Cyclooctene	80	24	1	TBHP/-/CH ₃ CN	77.5	99	[61]
(R)-UiO-68-Fe	2,2-Dimethyl-2 <i>H</i> -chromene	−20	1	36	MesPhIO/-/CHCl ₃	84	86 ee	[68]
Cusalen@NH ₂ -MIL-101(Cr)	Styrene	80	1	6	TBHP/-/CH ₃ CN	98.78	89.58	[69]
[Zn ₄ O(L ⁵ Cu,Mn) ₃]	2,2-Dimethyl-2 <i>H</i> -chromene	−20	1	36	MesPhIO/-/CH ₂ Cl ₂	86	86 ee	[70]
PCN-224-Mn(tart)	Styrene	60 °C	1	4	O ₂ /IBA/CH ₃ CN	100	89	[71]

Table 3. Cont.

MOF	Substrate	Reaction Data			Oxidant/Cocatalyst/ Solvent ^a	Conversion %	Epoxide Selectivity%	Ref.
		T (°C)	P (atm)	Time (h)				
	<i>trans</i> -Stilbene	60 °C	1	4	O ₂ /IBA/CH ₃ CN	80	100	[71]
	1-Phenyl-1-cyclohexene	60 °C	1	4	O ₂ /IBA/CH ₃ CN	75	100	[71]
	1-Octene	60 °C	1	4	O ₂ /IBA/CH ₃ CN	70	100	[71]
TMU-16-NH ₂	Cyclohexene	60	1	40	TBHP/-/CHCl ₃	66	74	[57]
	Styrene	60	1	51	TBHP/-/CHCl ₃	88	98	[57]
	Cyclooctene	60	1	24	TBHP/-/CHCl ₃	83	83	[57]

^a sPhIO = 2-(*tert*-butylsulfonyl)iodosylbenzene; IBA = isobutylaldehyde; CHP = cumene hydroperoxide; TBHP = *tert*-butylhydroperoxide.

3. Epoxidation with MOF-Based Composites

One possible way to improve the chemical and mechanical stability of MOFs as potentially heterogeneous catalysts is their immobilization onto/into supports. In this contest, solid polymer, graphene, and inorganic particles [72] or inorganic polymers [73] are largely employed as supports.

To overcome the poor hydrostability of [Cu₃-BTC₂] [74], a porous dendrimer-like porous silica nanoparticles (DPSNs) has been utilized as a carrier to support Cu-BTC Nps. The nanocomposites DPSNs@Cu-BTC were prepared by growing Cu₂O NPs in the center-radial porous channels of DPSNs. After that, Cu₂O NPs were dissolved in the presence of acid, oxidant and 1,3,5-benzenetricarboxylic acid (H₃BTC) [75]. The obtained Cu-BTC NPs have shown limited growth and a uniform distribution without agglomeration. The small size of Cu-BTC NPs (40 ± 25 nm) is useful in the aerobic epoxidation of various cyclic olefins achieving high catalytic activity without by-products. Good yield and selectivity were detected with inert terminal linear alkenes. Otherwise, epoxidation of styrene only achieved 65% of conversion due to the kinetic instability of styrene oxide (Table 4) [76].

The amphiphilic MIL-101-GH, a porous hierarchical material, has been explored as catalyst for the biphasic epoxidation reaction of 1-octene with H₂O₂. MIL-101-GH hydrogel was obtained by dispersing MIL-101 nanoparticles homogeneously in aqueous graphene oxide (GO) solutions. The TS-1 catalyst, commercially used in this biphasic reaction, was then introduced in MIL-101-GH. The resulting system, MIL-101-GH-TS-1, overcame the lower activity toward olefin epoxidation of TS-1, and the amphiphilic MIL-101-GH increased the contact areas of TS-1 with both H₂O₂ and 1-octene. The catalytic performance of MIL-101-GH-TS-1 has been much higher than that of single TS-1 and the 1,2-epoxyoctane was obtained without other by-products [77].

Polyoxometalate-based (POMs) heterogeneous catalysts are attractive species in the catalytic epoxidation of olefin. They have got great catalytic activity, selectivity, and easy separation but their leaching mainly due to the strong complexing capability of solvent and H₂O₂ oxidants, represents the major obstacle in the possible applications [78,79]. To overcome the stability issue of POMs, the polyoxomolybdic cobalt (CoPMA) and polyoxomolybdic acid (PMA) species were incorporated into UiO-bpy, a Zr-based MOFs, through self-assembly process under solvothermal condition [80]. CoPMA@UiO-bpy showed the highest catalytic activity for cyclooctene oxidation with H₂O₂ and also for the oxidation of styrene and 1-octene with O₂ as oxidant and *tert*-butyl hydroperoxide (t-BuOOH) as initiator. This is due to the uniform distribution and better immobilization of POM clusters within the size-matched cages of Zr-MOFs owing to the presence of bipyridine groups in the UiO-bpy framework. It is noteworthy that CoPMA@UiO-bpy shows excellent recyclability and stability against the leaching of active POM species.

Composite material has been obtained by encapsulating H₅-PMo₁₀V₂O₄₀ polyoxometalates (POMs) and 1-octyl-3-methylimidazolium bromide, ionic liquids (ILs), in the mesoporous cages and large surface area of MIL-100 (Fe). The synergic effect of ILs, Lewis and Brønsted acid sites in both PMo₁₀V₂ species and MOF created a PMo₁₀V₂-ILs@MIL-100(Fe) hybrid with significant catalytic properties in cycloolefins epoxidation. Indeed,

the PMo10V2 was activated by the imidazolium cations originated from ILs and the incorporation on MIL-100(Fe) prevented the leaching of POMs [81]. This composite is easily regenerated for 12 cycles without loss catalytic performance [82].

MIL-100(Fe) combined with the polyoxometalate $(C_{16}H_{36}N)_6K_2[\gamma-SiW_{10}O_{36}]$ has been reported to catalyse epoxidation of 3Z,6Z,9Z-octadecatriene to the corresponding 6,7-epoxide with high site selectivity (82.35%). The conversion catalysed by POM/MIL-100(Fe) exhibits a greater performance when the MOF contains unsaturated Lewis acid iron ions [83]. The main product of this epoxidation is a sex pheromone of *E. obliqua* Prout and can be potentially used in pest insect control with environmental friendliness.

Two POMs-based MOFs, $[Cu_6(bip)_{12}(PMo^VI_{12}O_{40})_2(PMo^VMo^VI_{11}O_{40}O_2)] \cdot 8H_2O$ and $[Co_3^{II}Co_2^{III}(H_2bib)_2(Hbib)_2(PW_9O_{34})_2(H_2O)_6] \cdot 6H_2O$ ($H_2bip = 1,3$ -bis(imidazolyl)propane; $bib = 1,4$ -bis(imidazol)butane)), have been fabricated using a flexible N-containing bidentate ligands via hydrothermal condition. They have been employed in the catalytic processes for selective alkene epoxidation and recycled four times without loss of quality (Figure 7) [84].

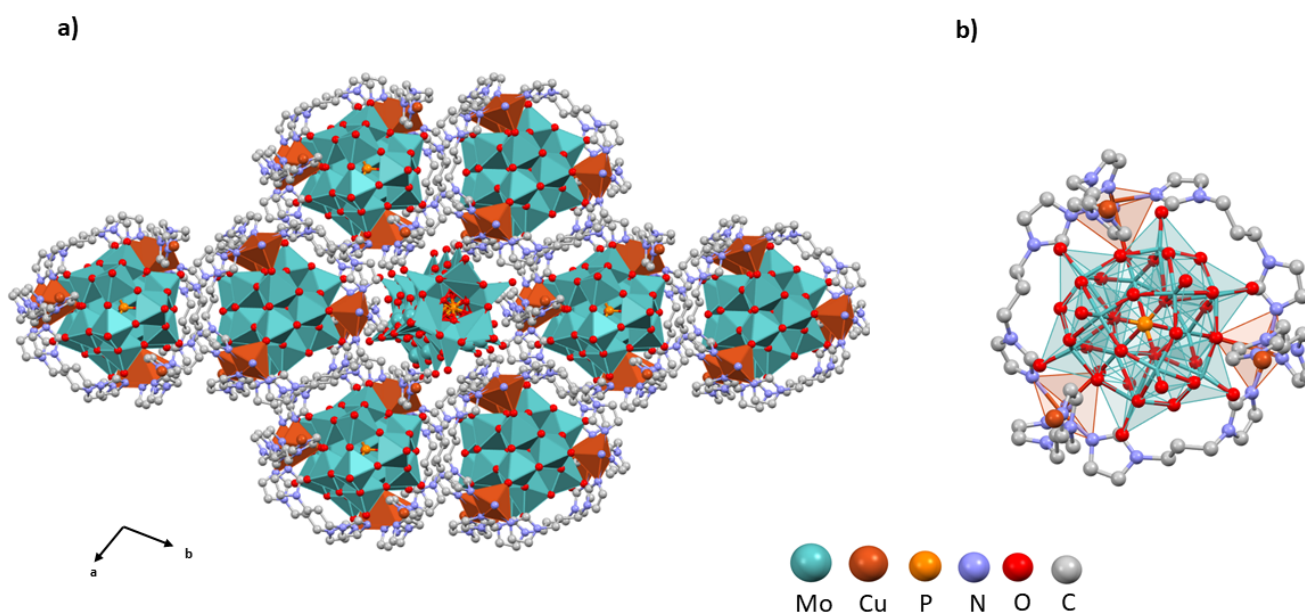


Figure 7. (a) The 2D structure of $[Cu_6(bip)_{12}(PMo^VI_{12}O_{40})_2(PMo^VMo^VI_{11}O_{40}O_2)] \cdot 8H_2O$; (b) the coordination environment of the Cu(II) cations. Hydrogens and hydroxyls are omitted for clarity. Light-blue polyhedral correspond to the (PMo_{12}) polyanion.

Metal nanoparticles can grow without agglomeration in a porous matrix to produce a stable and active heterogeneous catalyst. Pd NPs have been loaded on the pre-synthesized UiO-66-NH₂ using a simple solution impregnation method and NaBH₄ reduction. The amino groups in the linkers allow a strong interaction with Pd (II) ions which is essential to yielding well-dispersed Pd/UiO-66-NH₂ catalyst. The experiments suggest that the best catalytic activity for styrene epoxidation has been found under Pd NPs loadings of 3.69 wt% [85].

A dually functionalized catalytic system for the tandem H₂O₂-generation/alkene-oxidation reaction has been realized. A microcrystal of UiO-66-NH₂ has been used as a platform to encapsulate Au and Pd metal NPs and later Pd/Au@UiO-66-NH₂ surfaces have been post-synthetically modified with a (sal)Mo^{VI} (sal = salicyaldimine) molecular epoxidation catalyst. The porosity of Pd@UiO-66-sal(Mo) allows H₂ and O₂ gases to come into contact with the encapsulated NPs to generate H₂O₂. The synergic effect of the generated H₂O₂ and (sal)Mo^{VI} in a MOF enhanced epoxide productivity reducing alkene hydrogenation side reaction. This study showed that (sal)Mo moieties in Pd@UiO-66-NH₂

epoxidize cis-cyclooctene substrate faster, leading to the more effective usage of the H₂O₂ oxidant [86].

Systems composed of a magnetic uniform Fe₃O₄(PAA) microspheres core and of a copper-doped MOF shell demonstrated an easily catalyst recovery approach improving turnover number and turnover frequency. In addition, these magnetic core-shell heterogeneous catalysts improve both stability of the metal active site and dispersity of catalyst materials reducing the metal leaching. Two interesting magnetic core-shell copper-doped catalysts, Fe₃O₄@P4VP@ZIF-8 and Fe₃O₄/Cu₃(BTC)₂ have been prepared by combining the solvothermal method with layer-by-layer assembly. Initially, monodispersed PAA-modified Fe₃O₄ particles were synthesized by solvothermal methods [87]. In the case of Fe₃O₄/Cu₃(BTC)₂, Fe₃O₄ particles were alternately immersed in solutions containing Cu(CH₃COO)₂·H₂O and H₃BTC such that Cu₃(BTC)₂ nanocrystals grow layer-by-layer on the surface of PAA-modified Fe₃O₄ particles. This nanosized porous structure increases the contact between the Cu(II) active sites present in the Cu₃(BTC)₂ shell and the catalytic substrates [88]. In Fe₃O₄@P4VP@ZIF-8 catalyst, on the other hand, the Fe₃O₄(PAA) core has been coated with P4VP middle layer to adsorb a large number of Zn²⁺ for the growth of the ZIF-8 shell thickness on the surface of the core-shell Fe₃O₄(PAA)@P4VP. Then, the Zn²⁺ ions were partially substituted by Cu²⁺ ions in the ZIF-8 shell framework. The ions exchange allowed a well-dispersed copper active site in the resulting copper-doped ZIF-8 structure, avoiding their leaching [89].

Aerobic epoxidation of cyclic olefins (e.g., cyclohexene, norbornene) using both magnetic core-shell copper-doped Fe₃O₄@P4VP@ZIF-8 and Fe₃O₄/Cu₃(BTC)₂ as heterogeneous catalyst achieved high conversion and selectivity (99%) in the formation of the epoxide under mild reaction conditions. Epoxidation of styrene by using Fe₃O₄@P4VP@ZIF-8 as a catalyst has brought only 54% selectivity of the desired epoxide owing to the kinetic instability of styrene oxide and its oxidation into benzaldehyde [90].

A series of Zr-based core-shell MOF composites with mesoporous cores and microporous shells have been synthesized by solvothermal under kinetic control. PCN-222(Fe) crystals have been synthesized and used as seed crystals to grow the Zr-BPDC(UiO-67) crystals. Meso- and micro-porosity inside of PCN-222(Fe)@Zr-BPDC(UiO-67) drives the catalytic performances for olefin epoxidation reaction [91]. Indeed, the core MOF with Fe-porphyrin moieties represents the catalytic center, while the shell controls the selectivity of the substrate through tuneable pore size. This size-selective catalyst showed almost complete conversions for small olefins.

Table 4. MOF-based composites for epoxidation reaction.

MOF	Substrate	Reaction Data			Oxidant/Cocatalyst/ Solvent ^a	Conversion %	Epoxide Selectivity%	Ref.
		T (°C)	P (atm)	Time (h)				
DPSNs@Cu-BTC	Cyclooctene	40	1	4	O ₂ /TMA/CH ₃ CN	99	99	[75]
	Styrene	40	1	6	O ₂ /TMA/CH ₃ CN	62	65	[75]
Fe ₃ O ₄ @P4VP@ZIF-8	Cyclohexene	60	1	12	O ₂ /TMA/CH ₃ CN	99	99	[90]
	Cyclooctene							
	Norbornene							
Fe ₃ O ₄ /Cu ₃ (BTC) ₂	Cyclohexene	40	1	6–8	O ₂ /IBA/CH ₃ CN	99	99	[88]
	Cyclooctene							
	Norbornene							
PCN-222(Fe)@Zr-BPDC(UiO-67)	Styrene	40	1	6–8	O ₂ /IBA/CH ₃ CN	99	84	[88]
	1-Hexene							
	Cyclopentene							
CoPMA@UiO-bpy	Cyclohexene	r.t	1	12	PhIO/-/CH ₃ CN	99	-	[91]
	Cyclooctene							
	Styrene							
PMo10V2-ILs@MIL-100(Fe)	Cyclooctene	70	1	6	H ₂ O ₂ /-/CH ₃ CN	91	99	[80]
	Styrene							
PMo10V2-ILs@MIL-100(Fe)	Cyclooctene	80	1	6	O ₂ /t-BuOOH/-	80	56	[80]
	Cyclohexene							
PMo10V2-ILs@MIL-100(Fe)	Cyclohexene	60	1	4	H ₂ O ₂ /-/CH ₃ CN	92	93	[91]
	Cyclooctene							

Table 4. Cont.

MOF	Substrate	Reaction Data			Oxidant/Cocatalyst/ Solvent ^a	Conversion %	Epoxide Selectivity%	Ref.
		T (°C)	P (atm)	Time (h)				
[Cu ₆ (bip) ₁₂ (PMoVI ₁₂ O ₄₀) ₂ (PMoVMoVI ₁₁ O ₄₀ O ₂)]·8H ₂ O	Cyclooctene	20	1	4	H ₂ O ₂ /tBuOH/CH ₃ CN	>99	74.1	[84]
	1–Hexene	20	1	4	H ₂ O ₂ /tBuOH/CH ₃ CN	>99	91.9	[84]
	1–Octene	20	1	4	H ₂ O ₂ /tBuOH/CH ₃ CN	>99	71.5	[84]
Pd/UiO-66-NH ₂	Styrene	80	1	12	N ₂ /TBHP/CH ₃ CN	90.8	96.5	[85]
[Co ^{II} ₃ Co ^{III} ₂ (H ₂ bib) ₂ (Hbib) ₂ (PW ₉ O ₃₄) ₂ (H ₂ O) ₆]·6H ₂ O	Cyclohexene	20	1	4	H ₂ O ₂ /tBuOH/CH ₃ CN	72.9	95.3	[84]
	1–Hexene	20	1	4	H ₂ O ₂ /tBuOH/CH ₃ CN	>99	85.9	[84]
	1–Octene	20	1	4	H ₂ O ₂ /tBuOH/CH ₃ CN	95.5	70.1	[84]
POM/MIL-100(Fe)	3Z,6Z,9Z- Octadecatriene	40	1	24	H ₂ O ₂ /-/CH ₃ CN	30	82	[83]
MIL-101-GH-TS-1	Octane	40	1	12	H ₂ O ₂ (30%)/-/-	15	-	[77]
Pd@UiO-66-sal(Mo)	cis-Cyclooctene	r.t	1	6	H ₂ O ₂ /CH ₃ OH/H ₂ O	-	-	[86]

^a tBuOH = *tert*-butyl alcohol; TMA = trimethylacetaldehyde; IBA = isobutyraldehyde.

4. CO₂ Epoxide Cycloaddition to Cyclic Carbonates

Cycloaddition reaction of CO₂ with epoxides represents one of the most economically efficient approaches in the production of cyclic organic carbonates with relevant applications ranging from raw materials in the pharmaceuticals industry, polar aprotic solvents, electrolytes in lithium batteries, lubricants, precursors for polycarbonate materials, and other fine chemicals.

CO₂, being a C1 feedstock has, in fact, a high potential from the chemical point of view [92]. CO₂ can be employed in the highly atom-economical acid-catalysed epoxides cycloaddition to give cyclic organic carbonates, relevant species for industrial applications [93]. The cyclic carbonates (OCs) have been also used as intermediates for engineered polymers, as a lubricant (in 1987 Agip Petroli added dialkylcarbonates as lubricant in a formulation of semisynthetic gasoline engine oil components), and more recently found application in varnish production, green solvents or electrolytes in lithium-ion batteries.

The CO₂ cycloaddition mechanism involves an acid catalyst (Lewis or Brønsted acid) that coordinates to the epoxide substrate activating it toward nucleophilic attack by the co-catalyst (e.g., typically a tetraalkylammonium halide). The resulting halo-alkoxide intermediate reacts with carbon dioxide to generate the cyclic carbonate and subsequently regeneration of both catalyst and co-catalyst [93].

The CO₂ fixation reaction catalysed by homogeneous or heterogeneous catalysts has been extensively investigated, however some drawbacks remain. Differently from the homogeneous, heterogeneous catalysts (e.g., ionic liquid-supported solids [94–96], polymers [96,97], and porous organic frameworks [98]) have the advantages of easy separation and regeneration of the catalyst, but they often required rough conditions (high temperature, pressure, and time) due to a lack of accessible surface area for accelerating interactions of CO₂ and reagents with active sites. Therefore, the high surface area, tunability, and CO₂ sorption capacity of MOFs can be beneficial for improving the efficiency of the CO₂ cycloaddition reaction. Lewis acid metal centers and Brønsted acid groups in MOFs can promote the activation of the epoxide ring, while the functional groups in the ligands can act as Lewis/basic sites improving not only the CO₂ affinity inside the pore but also can fulfil the role of co-catalyst (Figure 8) [99].

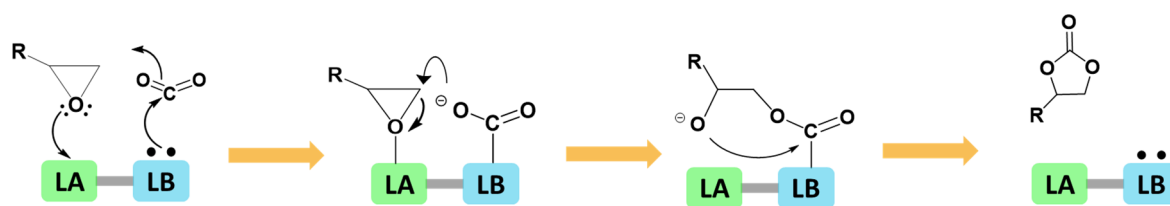


Figure 8. Proposed mechanism for the cycloaddition of CO₂ to epoxide with Lewis acid and base catalysts.

The Hf-cluster-based NU-1000 (Hf-NU-1000) demonstrated excellent catalytic activity, greater than the Zr-cluster-based NU-1000 under the same mild reaction conditions [100]. Indeed, the presence of high density stronger acidic Brønsted sites, due to stronger M–O bonds, gave a complete and quantitative conversion of styrene oxide and propylene oxide to form cyclic carbonates. Moreover, high yields have been detected for the cycloaddition reaction of CO₂ with industrially important epoxide divinylbenzene dioxide (DVBDO) [101].

Large pores in the MOFs, easily functionalized by polar groups, can promote CO₂ fixation in a short reaction time under ambient CO₂ pressure and moderate temperature without the use of solvent. Within the mesoporous M-MOF-184 series (M = Co, Ni, Mg, Zn), Zn-MOF-184 achieved efficient catalysis performances to convert CO₂ to cyclic carbonates under ambient conditions for several epoxy substrate, due to the presence of high concentration of accessibly acidic metals, basic 2-oxidobenzoate anion sites and to the high polarity induced by C≡C bonds and π systems from the phenyl rings in the linkers. Low conversion has been detected for larger epoxides due to limit diffusion into the MOF pores of reactants toward the active sites [102]. The hydrothermally synthesized flexible Zn-based {[Zn₂(TBIB)₂(HTCPB)₂]·9DMF·19H₂O}_n, has been synthesized employing two types of large linkers 1,3,5-tri(1H-benzo[d]imidazol-1-yl)benzene (TBIB) and 1,3,5-tris(4'-carboxyphenyl-)benzene (H₃TCPB). A porous structure with 1D channels was generated via noncovalent supramolecular interactions between the layers. The presence of free protonated carboxylic acid groups (–COOH), carbonyl groups (–C=O), and the presence of Lewis basic sites from the rich N-containing TBIB on the surface pores enhance the selectivity toward CO₂. Moreover, the COOH group helps in catalysing the CO₂ cycloaddition reaction efficiently through noncovalent interaction with the epoxide substrate, followed by ring-opening upon nucleophilic attack of co-catalyst [103].

Excellent conversions of epichlorohydrin and 2-vinyloxirane have been obtained using as heterogeneous catalyst [Zn₄OL₄]_n based on the meta-substituted 2,2',6,6'-tetramethoxy-4,4'-biphenyldicarboxyate ligand [39].

Zeolitic imidazolate frameworks are known for their high CO₂ solubility and capture ability [104], especially the chloro-functionalized ZIF-95 [105]. The CO₂ cycloaddition to propylene oxide by using ZIF-95 and a quaternary ammonium salt as cocatalyst procured over 99% selectivity to the desired propylene carbonate product under moderate conditions [106]. Also the imidazolate-containing species Im-UiO66(Zr)MOF reacts with methyl iodine to produce (I[−])MeIm-UiO-66 that demonstrate efficiency in the CO₂ cycloaddition reaction toward a broad range of substrates, in this case without the addition of co-catalyst [107].

Conversely, imidazolium-based IL units were grafted and immobilized into UiO-67 via direct ligand functionalization that, considering the post synthetic approach, is a quantitative method. The obtained species show a high density of IL sites. UiO-67-IL converts epichlorohydrin substrate in 95% yield under co-catalyst and solvent-free conditions. The yield increases to 99% in a shorter time when TBAB was employed (TBAB = tetrabutylammonium bromide) [108] (Table 5).

UiO-66-NH₂ pores were modified with ILs such as methylimidazolium bromide and methylbenzimidazolium bromide by coupling reactions, to generate ILA@U6N and ILB@U6N MOFs. The Lewis acid sites (for activation of the epoxide) and the IL functional sites (for epoxide ring-opening) efficiently catalyse the epichlorohydrin conversion under mild conditions [109].

A linear ionic polymer was inserted inside the MIL-101(Cr) via in situ polymerization to form polyILs@MIL-101(Cr) stable heterogeneous composites. This polyILs@MIL-101 is able to catalyse the CO₂ cycloaddition reaction with various epoxides with good to excellent conversions, including terminal epoxides with both electron-withdrawing and electron-donating substituents without the need of co-catalyst [110].

A new multimodal catalytic system has been designed via two steps post-synthetic modification of the metal nodes in the NU-1000 framework. A tandem functionalization was performed starting from the incorporation of *ortho*-, *meta*-, and *para*-pyridinecarboxylic acids into the framework of NU-1000(M), then the pyridine moieties were alkylated with various haloalkanes (CH₃I, C₄H₉I, C₄H₉Br, and C₆H₄F₉I) to introduce co-catalyst moieties near to the inorganic node [111]. Among catalysts, NU-1000(Zr) functionalized with 4-PyCOOH and CH₃I, i.e., SALI-4-Py-I-(Zr), showed the highest styrene carbonate yield without co-catalyst, the epoxy ring being activated upon coordination to Zr⁴⁺ center (Lewis acid site) and the halogen anion opening the epoxy ring by nucleophilic attack on the less sterically hindered carbon atom [111].

Two 3D metal-cyclam-based zirconium MOFs [Zr₆(μ₃-OH)₈(OH)₈(M-L)₄] (where M = Cu(II) or Ni(II), L1 = 6,13-dicarboxy-1,4,8,11-tetraazacyclotetradecane) were prepared, namely VPI-100 (Cu) and VPI-100 (Ni) (VPI = Virginia Polytechnic Institute), respectively. A two-step solvothermal synthesis has been necessary to build the MOFs. Initially, a zirconium-oxo cluster was assembled, then cyclam was added. The presence of accessible Cu²⁺/Ni²⁺ metal active sites in the metallocyclams and of the coordinatively unsaturated Zr⁴⁺ sites in the equatorial plane of the Zr₆ cluster in VPI-100 improved their catalytic activity toward CO₂ cycloaddition to various organic epoxides [112].

Another strategy developed to increase the catalytic performances is based on the incorporation of an amine group in MOFs. Essentially, the amino group has the dual advantage of acting as an electron donor (Lewis base) toward CO₂ and increasing the local concentration of CO₂ near catalytic centres through a high CO₂ adsorption [113,114].

The amine-functionalized NH₂-MIL-101(Al) has been synthesized using a solvothermal or microwave method and its catalytic activity in the solvent-free cycloaddition of CO₂ to styrene oxide achieved nearly total conversion and selectivity in 96% yield, with a TOF of 23.5 h⁻¹ [115]. The coordinatively unsaturated aluminium centers present in the SBUs (Lewis acidic sites) bind the epoxides and activate them toward ring-opening, this step is immediately followed by the attack of the bulky bromide ions of TBAB. The pendant amino groups polarize the CO₂ molecules, through the nucleophilic attack at the carbon atom, and facilitate CO₂ insertion and cycloaddition (Figure 9). During the catalytic reaction, the micro and mesoporous of the framework facilitate the diffusion of substrates and reactants to enhance their interactions [116].

Recently, the acid-base pair UiO-66-NH₂ has been used to synthesize bio-based five-membered cyclic carbonate from vegetable oil methyl ester by CO₂ fixation. At first, 95% of double bonds in the O-acetyl methyl ricinoleate starting material were converted to epoxide through an enzyme-catalyzed process. Then, the cycloaddition of epoxy fatty acid methyl esters was performed in the presence of UiO-66-NH₂ as catalyst and TBAB as co-catalyst for CO₂ fixation. At 120 °C under 3 MPa CO₂ pressure for 12 h, the reaction conversion reached 94.4% [117] (Table 5).

A series of diamino-tagged zinc bipyrazolate MOFs have been investigated as heterogeneous catalyst in the reaction of CO₂ with the epoxides epichlorohydrin and epibromohydrin to give the corresponding cyclic carbonates at 393 K and pCO₂ 5 bar under relatively mild conditions (solvent and co-catalyst-free) [118]. The presence of amino group in the MOFs pores increased the CO₂ storage capacity as well as the catalytic performances. The epoxide has been activated through halogen-amine interaction which was observed in structure of the [epibromohydrin@Zn(3,3'-(NH₂)₂BPZ)] adduct. The isomeric Lewis basic site (NH₂) in Zn(3,5 NH₂-Bpz) (64% yield) improves more than twice the catalytic transformation of epichlorohydrin compared to its mono(amino) parent Zn(BPZNH₂) (32% yield) [118].

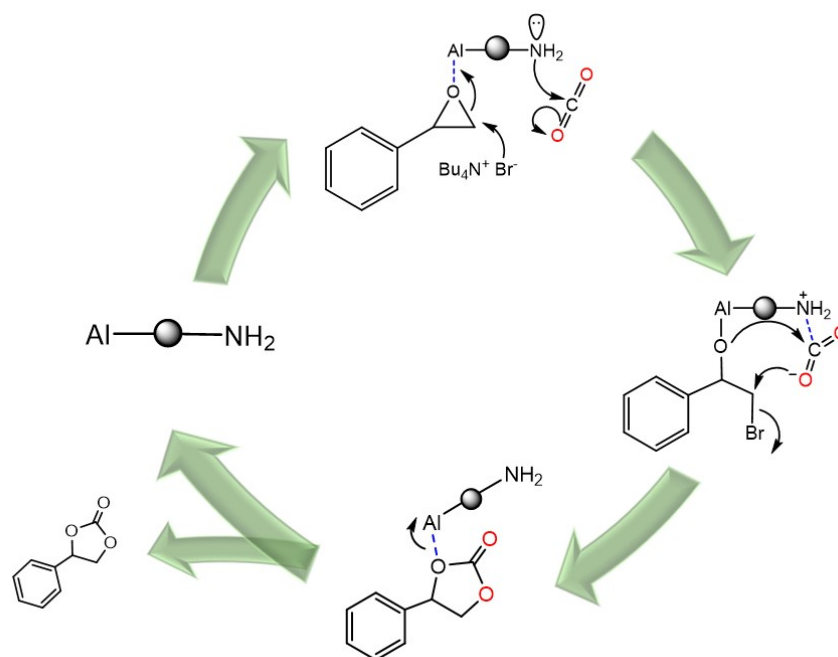


Figure 9. Proposed mechanism for the cycloaddition of styrene oxide and CO₂ using tetrabutylammonium bromide.

Post-synthetic metalation of organic linkers is employed strategically to tailor the MOFs' properties. In Hf-Bipy-UiO-67, the 2,2-bipyridine-5,5-dicarboxylate ligand was grafted with Mn(OAc)₂ and the resulting Hf-Bipy-UiO-67(Mn(OAc)₂) showed that synergy of the binary Lewis acid function significantly enhances the CO₂ uptake capacity and catalytic performance of the cycloaddition reaction under mild conditions [119].

Vanadium chlorides have been used to produce the post-metallated Zr-based MOF-VCl3 and MOF-VCl4, with biphenyl-4,4'-dicarboxylic acid, and 2,2'-bipyridine-5,5'-dicarboxylic acid, respectively, which provide Lewis basic sites. Their high catalytic activity in the CO₂ cycloaddition to various organic epoxides was attributed to the accessible Cu²⁺/Ni²⁺ metal active sites in the metallocyclams and the presence of coordinatively unsaturated Zr⁴⁺ sites in the equatorial plane of the Zr₆ cluster in VPI-100 MOFs [112].

UiO-type MOFs become susceptible to water and alkaline solution when the length of the carboxylic linker increase. A series of UiO-type MOF named ZSF, incorporating chiral metallosalen as linker has been produced. The chemically stable ZSF-1 MOF, synthesized by dissolving a mixture of ZrCl₄, Cy-salen-Ni, and modulators (trifluoroacetic acid), showed excellent catalytic performance for the conversion of CO₂ with epoxides into cyclic carbonates. The tetrahedral cages of ZSF-1 decorated with salen-Ni moieties entrap efficiently CO₂ and activate the substrate. ZSF-1 catalyses efficiently the asymmetric cycloaddition of CO₂ with styrene oxide giving 94% yield of the resulting cyclic carbonate [120]. With other epoxides, specifically epichlorohydrin, the catalytic activity of ZSF-1 increases until to 99% of conversion thanks to the presence of electron-withdrawing Cl group, which promotes the nucleophilic attack of Br⁻ during the ring-opening process.

The chiral PCN-224-Mn(tart) (see Section 2.3) has been used in asymmetric CO₂ cycloaddition to styrene epoxide, its derivative showing conversions of 96% and 87%, respectively. The missing-linker defects in the Zr cluster and in the Mn center are Lewis acids inducing catalytic ability into the framework for CO₂ chemical fixation. In addition, the auxiliary chiral tartrate anions, and the co-catalyst (Bu₄NBr) act as nucleophiles generating a chiral epoxide, semi-intermediate, starting from prochiral styrene substrate. The CO₂ addition leads asymmetrically to cyclic carbonate with a high ee, and it is related to the interaction of the chiral centers and substrate pro R/S face. Moreover, catalytic reactions with PCN-224-Mn(tart) were performed at low energy and ambient pressure and temperature [71].

Table 5. MOF-based composites for cycloaddition reaction.

MOF	Substrate	Reaction Data			Cocatalys ^a	Conversion %	Cyclic Carbonate Selectivity%	Ref.
		T (°C)	CO ₂ P (atm)	Time (h)				
Hf-NU-1000	Styrene epoxide	r.t.	1	56	TBAB	100	100	[101]
	Propylene oxide	r.t.	1	26	TBAB	100	100	[101]
	Epoxide divinylbenzene dioxide	r.t.	1	19	TBAB	100	100	[101]
PCN-224-Mn(tart)	Styrene epoxide	60	1	15	TBAB	96 94 ee (S)	100	[71]
	(2,3-Epoxypropyl)benzene	60	1	15	TBAB	87 90 ee (S)	100	[71]
	Propylene oxide	60	1	15	TBAB	99 98 ee (S)	100	[71]
	1,2-Epoxybutane	60	1	15	TBAB	91 97 ee (S)	100	[71]
	1,2-Epoxyoctane	60	1	15	TBAB	78 96 ee	100	[71]
polyILs@MIL-101(Cr)	1-Butene oxide	45	1	48	-	94	100	[110]
	1,2-Epoxyhexane	70	1	24	-	89	100	[110]
	3-Hydroxy-1,2-epoxypropane	70	1	24	-	>99	100	[110]
	1,2-Epoxy-3-phenoxypropane	70	1	24	-	95	100	[110]
NH ₂ -MIL-101(Al)	Styrene oxide	120	18	6	TBAB	93.6	99	[115]
UiO-66-NH ₂	Epoxy fatty acid methyl ester	120	30	12	TBAB	94	80	[117]
ILB@U6N	Epichlorohydrin	80	118	4	-	94	99	[109]
(I ⁻)Meim-UiO-66	Epichlorohydrin	120	1	24	-	100	93	[107]
VPI-100 (Ni)	Epichlorohydrin	90	10	6	TBAB	96	-	[112]
VPI-100 (Cu)	Epichlorohydrin	90	10	6	TBAB	94	-	[112]
[Zn ₄ OL ₄] _n	Epichlorohydrin	50	1	4	-	96	99	[107]
	2-Vinyloxirane	50	1	4	-	99	81	[107]
Hf-Bipy-UiO-67(Mn(OAc) ₂)	Epichlorohydrin	25	1	12	TBAB	83.2	99	[119]
Zn-MOF-184	Styrene oxide	80	1	6	TBAB	96	85	[102]
	Propylene oxide	80	1	6	TBAB	100	75	[102]
	Epichlorohydrin	80	1	6	TBAB	100	70	[102]
	Cyclohexene oxide	80	1	6	TBAB	69	85	[102]
SALI-4-Py-I-(Zr),	Styrene oxide	80	4	4	-	99	98	[111]
ILA@U6N	Epichlorohydrin	80	118	4	-	65	99	[109]
UiO-67-IL	Epichlorohydrin	90	1	3	TBAB	99	100	[108]
	Epichlorohydrin	90	1	3	-	99	96	[108]
{[Zn ₂ (TBIB) ₂ (HTCPB) ₂]} 9DMF·19H ₂ O) _n	Epichlorohydrin	r.t.	1	24	TBAB	99	100	[105]
ZIF-95	Propylene oxide	120	118	24	TBAB	91	99	[106]
ZSF-1	Styrene oxide	100	1	20	TBAB	93	-	[120]
	Epichlorohydrin	100	1	20	TBAB	99	-	[120]
Zn(3,5-NH ₂ -Bpz)	Epichlorohydrin	120	5	24	-	98	50	[118]
Zn(BPZNH ₂)	Epichlorohydrin	120	5	24	-	96	33	[118]

^a TBAB = tetrabutylammonium bromide.

5. Conclusions

MOF-based catalysts are now a very promising class of compounds as they merge relevant characteristics of both homogeneous and heterogeneous catalysts. They can be easily modified by changing linkers substituents to increase affinity for reactants, or by growing the number of active catalytic sites.

In this review, we have explored the ability of MOFs, MOF nanocomposites and mixed metal species toward olefin epoxidation and carbon dioxide cycloaddition.

We have observed that the olefin conversion and the epoxide selectivity are strongly dependent on the metal nodes/clusters, Co and Cu species being the most efficient, in some cases as for the epoxidation of α -pinene by Co-MOF-150-2 a conversion and an epoxide selectivity close to 100% being found.

Mixed metal MOFs can be also successfully employed in styrene and cyclohexene epoxidation, the best results being obtained with Cu/Co, Mn/Cu, and Ni/V species.

Selected functional groups introduced in organic linkers can also act as catalytically active sites. Amino, pyridyl, amide and sulfonic acid groups, but also metalloporphyrins, vanadium and molybdenum acetylacetonate, tartaric acid, salen and analogous molecules can be inserted or deposited to obtain also greater selectivity. UiO-66, UiO67, and PCN-224, appropriately functionalized can induce a complete conversion and selectivity as in the case of the geraniol epoxidation.

MOF-based composites are often employed to increase the hydrostability of selected MOFs or to perform epoxidation also of specific substrates as norbornene or octadecatriene. Specifically, a porous dendrimer-like porous silica nanoparticles (DPSNs) used as a carrier to support Cu-BTC NPs overcame the poor hydrostability of [Cu₃-BTC₂] MOF achieving high catalytic activity without by-products under mild reaction conditions.

Finally, MOFs and MOF-based composites show a great efficiency toward CO₂ cycloaddition to epoxides, conversion being generally in the range 70–100% and selectivity close to 100%. The use of chiral ligands and amine-functionalized ligands seems to be very promising. The CO₂ binding mode can in fact open new strategies for activation of CO₂ and its transformation.

However, the low reactivity and inert nature of CO₂ make its incorporation and activation into organic substrates still a challenge. Currently, the heterogeneous MOFs-based catalysts, as well as the technical system, remain at the laboratory scale and that makes the costs of productions of these materials extremely pricey. It is desirable that the improvement of MOFs-based catalysts might lead to technically viable efficiencies to industrial production to allow their large-scale application, in the next future. This review clearly shows that MOFs are now perspective materials and valid candidates for catalytic epoxidation and CO₂ cycloaddition reactions.

Author Contributions: Conceptualization, A.T. and C.P.; methodology, A.T. and C.P.; software, A.T. and C.P.; validation, A.T. and C.P.; data curation, A.T. and C.P.; writing—original draft preparation, A.T. and C.P.; writing—review and editing, A.T. and C.P.; funding acquisition, C.P. All authors have read and agreed to the published version of the manuscript.

Funding: This research was funded by University of Camerino.

Conflicts of Interest: The authors declare no conflict of interest.

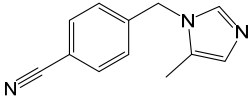
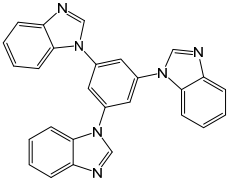
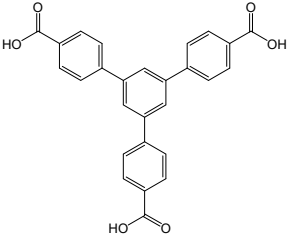
Abbreviations

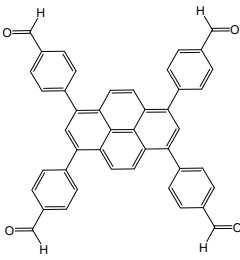
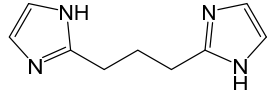
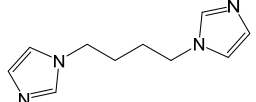
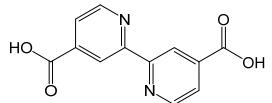
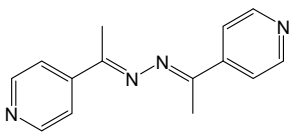
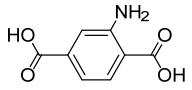
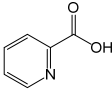
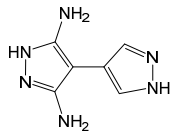
MOFs

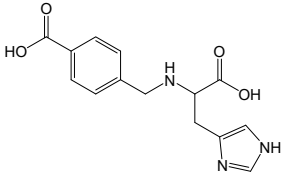
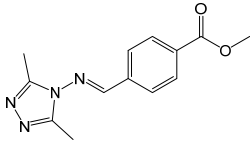
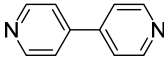
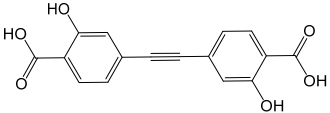
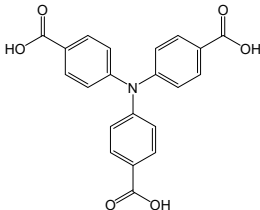
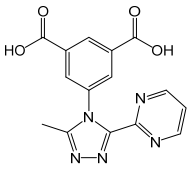
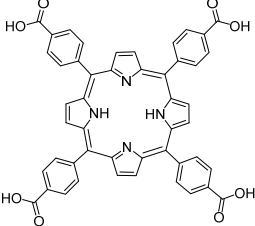
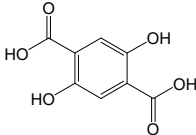
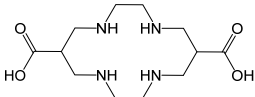
Co6-MOF-3	$[(\text{Co}_6(\text{OH})_6(\text{TCA})_2(\text{BPB})_3)_n]$
Co-MOF-150-2	$[\text{Co}(\text{BDC})_n]$
Cu _{0.25} -Co _{0.75} -MOF	$[(\text{Cu}_{0.25}\text{-Co}_{0.75})_3(\text{BTC})_2]_n$
HKUST-1	$[\text{Cu}_3(\text{BTC})_2]_n$
LaCoODA	$\{[\text{La}_2\text{Co}_3(\text{ODA})_6(\text{H}_2\text{O})_6] \cdot 12\text{H}_2\text{O}\}_n$
LaCuODA	$\{[\text{La}_2\text{Cu}_3(\mu\text{-H}_2\text{O})(\text{ODA})_6(\text{H}_2\text{O})_3] \cdot 3\text{H}_2\text{O}\}_n$

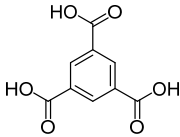
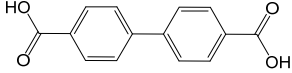
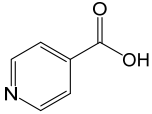
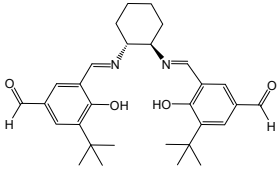
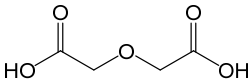
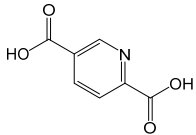
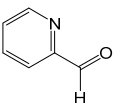
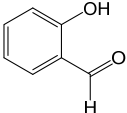
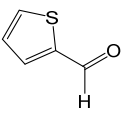
MIL-100(Fe)	$[\text{Fe}_3\text{O}(\text{OH})(\text{H}_2\text{O})_2(\text{BDC})_3]_n$
MIL-101	$[\text{Cr}_3\text{O}(\text{H}_2\text{O})_2\text{F}(\text{BDC})]_n$
$\text{Mn}_{0.1}\text{Cu}_{0.9}$ -MOF	$[(\text{Mn}_{0.1}\text{-Cu}_{0.9})_3(\text{BTC})_2]_n$
NENU-MV-1	$\{[\text{Ni}(4,4'\text{-bpy})_2]_2[\text{V}_7^{\text{IV}}\text{V}_9^{\text{V}}\text{O}_{38}\text{Cl}]\cdot(4,4'\text{-bpy})\cdot 6\text{H}_2\text{O}\}_n$
NH_2 -MIL-101(Al)	$[\text{Al}_3\text{O}(\text{OH})(\text{H}_2\text{O})_2(\text{BDCNH}_2)_3]_n$
NH_2 -MIL-101(Cr)	$\text{Cr}_3\text{O}(\text{H}_2\text{O})_2\text{F}(\text{NH}_2\text{-BDC})$
NTUZ30	$\{[\text{Co}_3(\mu_3\text{-OH})(\text{HBTC})(\text{BTC})_2\text{Co}(\text{HBTC})]\cdot(\text{HTEA})_3\cdot\text{H}_2\text{O}\}_n$
PCN-222	$[\text{Zr}_6(\mu_3\text{-OH})_8(\text{OH})_8(\text{TCPP})_2]_n$
PCN-224	$[\text{Zr}_6(\mu_3\text{-OH})_{12}(\text{OH})_{16}(\text{TCPP})_{1.5}]_n$
TMU-16- NH_2	$\{[\text{Zn}_2(\text{NH}_2\text{-BDC})_2(4\text{-bpdh})]\cdot 3\text{DMF}\}_n$
UiO-66	$[\text{Zr}_6\text{O}_4(\text{OH})_4(\text{BDC})_6]_n$
UiO-66- NH_2	$[\text{Zr}_6\text{O}_4(\text{OH})_4(\text{NH}_2\text{-BDC})_6]_n$
UiO-67	$[\text{Zr}_6(\mu_3\text{-O})_4(\mu_3\text{-OH})_4(\text{BPDC})_6]_n$
UiO-68	$[\text{Zr}_6(\mu_3\text{-O})_4(\mu_3\text{-OH})_4(\text{TPDC})_6]_n$
UiO-bpy	$[\text{Zr}_6\text{O}_4(\text{OH})_4(\text{bpy})_6]_n$
VPI-100(Cu)	$[\text{Zr}_6(\mu_3\text{-OH})_8(\text{OH})_8(\text{Cu-L1})_4]_n$
VPI-100(Ni)	$[\text{Zr}_6(\mu_3\text{-OH})_8(\text{OH})_8(\text{Ni-L1})_4]_n$
ZIF-67	$[\text{Co}(\text{MeIm})_2]_n$
ZIF-8	$[\text{Zn}(\text{MeIm})_2]_n$
ZIF-95	$[\text{Zn}(\text{cbIm})_2]_n$
Zn-MOF-184	$[\text{Zn}_2(\text{EDOB})]_n$
Zr-NU-1000	$([\text{Zr}_6(\mu_3\text{-O})_4(\mu_3\text{-OH})_4(\text{OH})_4(\text{H}_2\text{O})_4(\text{TBAPy})_2]_n$
ZSF-1	$[\text{Zr}_6\text{O}_4(\text{OH})_4(\text{metallosalen})_6]_n$
Hf-NU-1000	$[(\text{Hf}_6(\mu_3\text{-O})_4(\mu_3\text{-OH})_4(\text{OH})_4(\text{OH}_2)_4(\text{TBAPy})_2]_n$

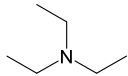
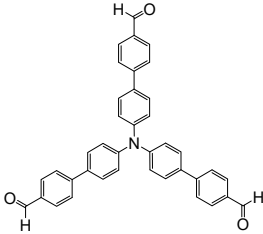
Appendix A. Chart of the MOF Linkers Present in This Review and Their Relative Abbreviations

Structural Formula	Name	Abbreviation
	1-(4-Cyanobenzyl)-5-methyl-1H-imidazole	cbIm
	1,3,5-tri(1H-Benzo[d]imidazol-1-yl)benzene	TBIB
	1,3,5-tris(4'-Carboxy-phenyl)-benzene	H ₃ TCPB

Structural Formula	Name	Abbreviation
	1,3,6,8-(p-Benzoate)pyrene	H ₄ TBAPy
	1,3-bis(Imidazolyl)propane	H ₂ bip
	1,4-bis(Imidazol)butane	bib
	2,2',6,6'-Tetramethoxy-4,4'-biphenyldicarboxylic acid	H ₂ L4
	2,2-Bipyridine-4,4'-dicarboxylic acid	H ₂ Bpy
	2,5-bis(4-Pyridyl)-3,4-diaza-2,4-hexadiene	4-bpdh
	2-Aminoterephthalic acid	H ₂ BDCNH ₂
	2-Methylimidazole	HmeIm
	2-Picolinic acid	PCA
	3,5-Diamino-4,4'-bipyrazole	H ₂ -NH ₂ -Bpz

Structural Formula	Name	Abbreviation
	4-((1-Carboxy-2-(1 <i>H</i> -imidazol-4-yl)ethylamino)methyl)benzoic acid	H ₂ L2
	4-(3,5-Dimethyl-4- <i>H</i> -1,2,4-triazol-4-yl) benzoate	Me ₂ trz-pba
	4,4'-Bipyridine	4,4'-bipy
	4,4'-(Ethyne-1,2-diyl)bis(2-hydroxybenzoic acid)	H ₄ EDOB
	4,4',4''-Tricarboxyltriphenylamine	H ₃ TCA
	5-(3-Methyl-5-(pyridine-4-yl)-4 <i>H</i> -1,2,4-triazol-4-yl) isophthalate	Me-4py-trz-ia
	5,10,15,20-Tetrakis(4-carboxyphenyl)porphyrin	H ₆ TCPP
	5-Dihydroxyterephthalic acid	H ₄ DHTA
	6,13-Dicarboxy-1,4,8,11-tetraazacyclotetradecane	L1

Structural Formula	Name	Abbreviation
	Benzene-1,3-5 tricarboxylic acid	H ₃ BTC
	Biphenyl-4,4'-dicarboxylic acid	H ₂ BPDC
	Imidazole	HIIm
	Isonicotinate	Ina
	N,N'-bis(3- <i>tert</i> -Butyl-5-(carboxy)salicylide	H ₄ L5
	Oxydiacetic acid	H ₂ ODA
	Pyridine-2,5-dicarboxylic acid	H ₂ pdc
	Pyridine-2-aldehyde	PI
	Salicylaldehyde	SA
	Thiophene-2-carbaldehyde	TC

Structural Formula	Name	Abbreviation
	Triethylamine	TEA
	Tris(4'-carboxybiphenyl)amine	H ₃ L3

References

- Batten, S.R.; Champness, N.R.; Chen, X.-M.; Garcia-Martinez, J.; Kitagawa, S.; Öhrström, L.; O'Keeffe, M.; Suh, M.P.; Reedijk, J. Terminology of metal–organic frameworks and coordination polymers (IUPAC Recommendations 2013). *Pure Appl. Chem.* **2013**, *85*, 1715–1724. [[CrossRef](#)]
- Furukawa, H.; Cordova, K.E.; O'Keeffe, M.; Yaghi, O.M. The Chemistry and Applications of Metal-Organic Frameworks. *Science* **2013**, *341*, 1230444. [[CrossRef](#)]
- Pettinari, C.; Marchetti, F.; Mosca, N.; Drozdov, A. Application of metal-organic frameworks. *Polym. Int.* **2017**, *66*, 93. [[CrossRef](#)]
- Li, H.; Eddaoudi, M.; O'Keeffe, M.; Yaghi, O. Design and synthesis of an exceptionally stable and highly porous metal-organic framework. *Nat. Cell Biol.* **1999**, *402*, 276–279. [[CrossRef](#)]
- Schaus, S.E.; Brandes, B.D.; Larrow, J.F.; Tokunaga, M.; Hansen, K.B.; Gould, A.E.; Furrow, M.E.; Jacobsen, E.N. Highly Selective Hydrolytic Kinetic Resolution of Terminal Epoxides Catalyzed by Chiral (salen)CoIII Complexes. Practical Synthesis of Enantioenriched Terminal Epoxides and 1,2-Diols. *J. Am. Chem. Soc.* **2002**, *124*, 1307. [[CrossRef](#)]
- Stock, N.; Biswas, S. Synthesis of Metal-Organic Frameworks (MOFs): Routes to Various MOF Topologies, Morphologies, and Composites. *Chem. Rev.* **2011**, *112*, 933. [[CrossRef](#)]
- Campagnol, N.; Souza, E.R.; De Vos, D.E.; Binnemans, K.; Franssaer, J. Luminescent terbium-containing metal–organic framework films: New approaches for the electrochemical synthesis and application as detectors for explosives. *Chem. Commun.* **2014**, *50*, 12545–12547. [[CrossRef](#)]
- Zhang, Y.; Bo, X.; Nsabimana, A.; Han, C.; Li, M.; Guo, L. Electrocatalytically active cobalt-based metal–organic framework with incorporated macroporous carbon composite for electrochemical applications. *J. Mater. Chem. A* **2014**, *3*, 732. [[CrossRef](#)]
- Masoomi, M.Y.; Morsali, A.; Junk, P.C. Rapid mechanochemical synthesis of two new Cd(ii)-based metal–organic frameworks with high removal efficiency of Congo red. *CrystEngComm* **2014**, *17*, 686. [[CrossRef](#)]
- Wu, J.-Y.; Chao, T.-C.; Zhong, M.-S. Influence of Counteranions on the Structural Modulation of Silver–Di(3-pyridylmethyl)amine Coordination Polymers. *Cryst. Growth Des.* **2013**, *13*, 2953. [[CrossRef](#)]
- Khan, N.A.; Jhung, S.H. Synthesis of metal-organic frameworks (MOFs) with microwave or ultrasound: Rapid reaction, phase-selectivity, and size reduction. *Coord. Chem. Rev.* **2015**, *285*, 11. [[CrossRef](#)]
- Maurin, G.; Serre, C.; Cooper, A.; Férey, G. The new age of MOFs and of their porous-related solids. *Chem. Soc. Rev.* **2017**, *46*, 3104–3107. [[CrossRef](#)]
- Murray, J.L.; Mircea, D.; Long, R.J. Hydrogen storage in metal–organic frameworks. *Chem. Soc. Rev.* **2009**, *38*, 1294–1314. [[CrossRef](#)]
- Sun, Y.; Zheng, L.; Yang, Y.; Qian, X.; Fu, T.; Li, X.; Yang, Z.; Yan, H.; Cui, C.; Tan, W. Metal–Organic Framework Nanocarriers for Drug Delivery in Biomedical Applications. *Nano-Micro Lett.* **2020**, *12*, 103. [[CrossRef](#)]
- Wang, H.-S. Metal–organic frameworks for biosensing and bioimaging applications. *Coord. Chem. Rev.* **2017**, *349*, 139–155. [[CrossRef](#)]
- Gao, X.; Dong, Y.; Li, S.; Zhou, J.; Wang, L.; Wang, B. MOFs and COFs for Batteries and Supercapacitors. *Electrochem. Energy Rev.* **2019**, *3*, 81–126. [[CrossRef](#)]
- Stavila, V.; Talin, A.A.; Allendorf, M.D. MOF-based electronic and opto-electronic devices. *Chem. Soc. Rev.* **2014**, *43*, 5994. [[CrossRef](#)]
- Xu, W.; Yaghi, O.M. Metal–Organic Frameworks for Water Harvesting from Air, Anywhere, Anytime. *ACS Central Sci.* **2020**, *6*, 1348–1354. [[CrossRef](#)]
- Zhang, L.; Li, H.; He, H.; Yang, Y.; Cui, Y.; Qian, G. Structural Variation and Switchable Nonlinear Optical Behavior of Metal–Organic Frameworks. *Small* **2021**, *17*, 2006649. [[CrossRef](#)]
- Dhakshinamoorthy, A.; Opanasenko, M.; Čejka, J.; Garcia, H. Metal organic frameworks as heterogeneous catalysts for the production of fine chemicals. *Catal. Sci. Technol.* **2013**, *3*, 2509–2540. [[CrossRef](#)]

21. Vanesa, C.-C.; Rosa, M.M.-A. Advances in Metal-Organic Frameworks for Heterogeneous Catalysis. *Recent Pat. Chem. Eng.* **2011**, *4*, 1–16.
22. Farrusseng, D.; Aguado, S.; Pinel, C. Metal-Organic Frameworks: Opportunities for Catalysis. *Angew. Chem. Int. Ed.* **2009**, *48*, 7502–7513. [[CrossRef](#)] [[PubMed](#)]
23. Chen, Y.; Ma, S. Biomimetic catalysis of metal-organic frameworks. *Dalt. Trans.* **2016**, *45*, 9744–9753. [[CrossRef](#)]
24. Corma, A.; García, H. Lewis Acids as Catalysts in Oxidation Reactions: From Homogeneous to Heterogeneous Systems. *Chem. Rev.* **2002**, *102*, 3837–3892. [[CrossRef](#)]
25. Kravchenko, D.E.; Tyablikov, I.A.; Kots, P.A.; Kolozhvari, B.A.; Fedosov, D.A.; Ivanova, I.I. Olefin Epoxidation over Metal-Organic Frameworks Modified with Transition Metals. *Pet. Chem.* **2019**, *58*, 1255–1262. [[CrossRef](#)]
26. Arai, H.; Uehara, K.; Kinoshita, S.I.; Kunugi, T. Olefin Oxidation-Mercuric Salt-Active Charcoal Catalysis. *Ind. Eng. Chem. Prod. Res. Dev.* **1972**, *11*, 308–312. [[CrossRef](#)]
27. Liniger, M.; Liu, Y.; Stoltz, B.M. Sequential Ruthenium Catalysis for Olefin Isomerization and Oxidation: Application to the Synthesis of Unusual Amino Acids. *J. Am. Chem. Soc.* **2017**, *139*, 13944–13949. [[CrossRef](#)]
28. Gao, J.; Bai, L.; Zhang, Q.; Li, Y.; Rakesh, G.; Lee, J.-M.; Yang, Y.; Zhang, Q. Co₆(μ₃-OH)₆ cluster based coordination polymer as an effective heterogeneous catalyst for aerobic epoxidation of alkenes. *Dalton Trans.* **2014**, *43*, 2559–2565. [[CrossRef](#)] [[PubMed](#)]
29. Zhang, X.; Zhang, Y.-Z.; Jin, Y.-Q.; Geng, L.; Zhang, D.-S.; Hu, H.; Li, T.; Wang, B.; Li, J.-R. Pillar-Layered Metal-Organic Frameworks Based on a Hexaprismane [Co₆(μ₃-OH)₆] Cluster: Structural Modulation and Catalytic Performance in Aerobic Oxidation Reaction. *Inorg. Chem.* **2020**, *59*, 11728–11735. [[CrossRef](#)]
30. Yu, F.; Xiong, X.; Huang, K.; Zhou, Y.; Li, B. 2D Co-based coordination polymer with a histidine derivative as an efficient heterogeneous catalyst for the oxidation of cyclohexene. *CrystEngComm* **2017**, *19*, 2126–2132. [[CrossRef](#)]
31. Zhang, H.; He, J.; Lu, X.; Yang, L.; Wang, C.; Yue, F.; Zhou, D.; Xia, Q. Fast-synthesis and catalytic property of heterogeneous Co-MOF catalysts for the epoxidation of α-pinene with air. *New J. Chem.* **2020**, *44*, 17413–17421. [[CrossRef](#)]
32. Lu, H.-S.; Bai, L.; Xiong, W.-W.; Li, P.; Ding, J.; Zhang, G.; Wu, T.; Zhao, Y.; Lee, J.-M.; Yang, Y.; et al. Surfactant Media To Grow New Crystalline Cobalt 1,3,5-Benzenetricarboxylate Metal-Organic Frameworks. *Inorg. Chem.* **2014**, *53*, 8529–8537. [[CrossRef](#)]
33. Sha, S.; Yang, H.; Li, J.; Zhuang, C.; Gao, S.; Liu, S. Co(II) coordinated metal-organic framework: An efficient catalyst for heterogeneous aerobic olefins epoxidation. *Catal. Commun.* **2014**, *43*, 146–150. [[CrossRef](#)]
34. Fu, Y.; Sun, D.; Qin, M.; Huang, R.; Li, Z. Cu(ii)-and Co(ii)-containing metal-organic frameworks (MOFs) as catalysts for cyclohexene oxidation with oxygen under solvent-free conditions. *RSC Adv.* **2012**, *2*, 3309–3314. [[CrossRef](#)]
35. Lashanizadegan, M.; Ashari, H.A.; Sarkheil, M.; Anafcheh, M.; Jahangiry, S. New Cu(II), Co(II) and Ni(II) azo-Schiff base complexes: Synthesis, characterization, catalytic oxidation of alkenes and DFT study. *Polyhedron* **2021**, *200*, 115148. [[CrossRef](#)]
36. Junghans, U.; Suttkus, C.; Lincke, J.; Lässig, D.; Krautscheid, H.; Gläser, R. Selective oxidation of cyclooctene over copper-containing metal-organic frameworks. *Microporous Mesoporous Mater.* **2015**, *216*, 151–160. [[CrossRef](#)]
37. Wang, B.; Jin, J.; Ding, B.; Han, X.; Han, A.; Liu, J. General Approach to Metal-Organic Framework Nanosheets With Controllable Thickness by Using Metal Hydroxides as Precursors. *Front. Mater.* **2020**, *7*, 37. [[CrossRef](#)]
38. Shi, D.; Ren, Y.; Jiang, H.; Cai, B.; Lu, J. Synthesis, Structures, and Properties of Two Three-Dimensional Metal-Organic Frameworks, Based on Concurrent Ligand Extension. *Inorg. Chem.* **2012**, *51*, 6498–6506. [[CrossRef](#)] [[PubMed](#)]
39. Li, J.; Ren, Y.; Qi, C.; Jiang, H. Fully meta-Substituted 4,4'-Biphenyldicarboxylate-Based Metal-Organic Frameworks: Synthesis, Structures, and Catalytic Activities. *Eur. J. Inorg. Chem.* **2017**, *11*, 1478–1487. [[CrossRef](#)]
40. Saha, D.; Gayen, S.; Koner, S. Cu(II)/Cu(II)-Mg(II) containing pyridine-2,5-dicarboxylate frameworks: Synthesis, structural diversity, inter-conversion and heterogeneous catalytic epoxidation. *Polyhedron* **2018**, *146*, 93–98. [[CrossRef](#)]
41. Dhakshinamoorthy, A.; Portillo, A.S.; Asiri, A.M.; Garcia, H. Engineering UiO-66 Metal Organic Framework for Heterogeneous Catalysis. *ChemCatChem* **2019**, *11*, 899–923. [[CrossRef](#)]
42. Vandichel, M.; Hajek, J.; Vermoortele, F.; Waroquier, M.; De Vos, D.E.; Van Speybroeck, V. Active site engineering in UiO-66 type metal-organic frameworks by intentional creation of defects: A theoretical rationalization. *CrystEngComm* **2014**, *17*, 395–406. [[CrossRef](#)]
43. Arrozi, U.S.; Wijaya, H.W.; Patah, A.; Permana, Y. Efficient acetalization of benzaldehydes using UiO-66 and UiO-67: Substrates accessibility or Lewis acidity of zirconium. *Appl. Catal. A Gen.* **2015**, *506*, 77–84. [[CrossRef](#)]
44. Zheng, H.-Q.; Zeng, Y.-N.; Chen, J.; Lin, R.-G.; Zhuang, W.-E.; Cao, R.; Lin, Z.-J. Zr-Based Metal-Organic Frameworks with Intrinsic Peroxidase-Like Activity for Ultradeep Oxidative Desulfurization: Mechanism of H₂O₂ Decomposition. *Inorg. Chem.* **2019**, *58*, 6983–6992. [[CrossRef](#)] [[PubMed](#)]
45. Liu, Y.; Klet, R.C.; Hupp, J.T.; Farha, O. Probing the correlations between the defects in metal-organic frameworks and their catalytic activity by an epoxide ring-opening reaction. *Chem. Commun.* **2016**, *52*, 7806–7809. [[CrossRef](#)] [[PubMed](#)]
46. Zalomaeva, O.V.; Evtushok, V.Y.; Ivanchikova, I.D.; Glazneva, T.S.; Chesalov, Y.A.; Larionov, K.P.; Skobelev, I.Y.; Kholdeeva, O.A. Nucleophilic versus Electrophilic Activation of Hydrogen Peroxide over Zr-Based Metal-Organic Frameworks. *Inorg. Chem.* **2020**, *59*, 10634–10649. [[CrossRef](#)] [[PubMed](#)]
47. Payne, G.B.; Deming, P.H.; Williams, P.H. Reactions of Hydrogen Peroxide. VII. Alkali-Catalyzed Epoxidation and Oxidation Using a Nitrile as Co-reactant. *J. Org. Chem.* **1961**, *26*, 659–663. [[CrossRef](#)]
48. Huang, K.; Yu, S.; Li, X.; Cai, Z. One-pot synthesis of bimetal MOFs as highly efficient catalysts for selective oxidation of styrene. *J. Chem. Sci.* **2020**, *132*, 139. [[CrossRef](#)]

49. Wang, F.; Meng, X.-G.; Wu, Y.-Y.; Huang, H.; Lv, J.; Yu, W.-W. A Highly Efficient Heterogeneous Catalyst of Bimetal-Organic Frameworks for the Epoxidation of Olefin with H₂O₂. *Molecules* **2020**, *25*, 2389. [[CrossRef](#)]
50. Santibáñez, L.; Escalona, N.; Torres, J.; Kremer, C.; Cancino, P.; Spodine, E. Cu^{II}- and Co^{II}-based MOFs: {[La₂Cu₃(μ-H₂O)(ODA)6(H₂O)₃·3H₂O]}_n and {[La₂Co₃(ODA)6(H₂O)₆·12H₂O]}_n. The Relevance of Physicochemical Properties on the Catalytic Aerobic Oxidation of Cyclohexene. *Catalysts* **2020**, *10*, 589. [[CrossRef](#)]
51. Tuci, G.; Giambastiani, G.; Kwon, S.; Stair, P.C.; Snurr, R.Q.; Rossin, A. Chiral Co(II) Metal–Organic Framework in the Heterogeneous Catalytic Oxidation of Alkenes under Aerobic and Anaerobic Conditions. *ACS Catal.* **2014**, *4*, 1032–1039. [[CrossRef](#)]
52. Otake, K.-I.; Ahn, S.; Knapp, J.; Hupp, J.T.; Notestein, J.M.; Farha, O.K. Vapor-Phase Cyclohexene Epoxidation by Single-Ion Fe(III) Sites in Metal–Organic Frameworks. *Inorg. Chem.* **2021**, *60*, 2457–2463. [[CrossRef](#)] [[PubMed](#)]
53. Ahn, S.; Thornburg, N.; Li, Z.; Wang, T.C.; Gallington, L.; Chapman, K.W.; Notestein, J.M.; Hupp, J.T.; Farha, O.K. Stable Metal–Organic Framework-Supported Niobium Catalysts. *Inorg. Chem.* **2016**, *55*, 11954–11961. [[CrossRef](#)]
54. Thornburg, N.E.; Nauert, S.L.; Thompson, A.B.; Notestein, J.M. Synthesis–Structure–Function Relationships of Silica-Supported Niobium(V) Catalysts for Alkene Epoxidation with H₂O₂. *ACS Catal.* **2016**, *6*, 6124–6134. [[CrossRef](#)]
55. Wang, S.; Liu, Y.; Zhang, Z.; Li, X.; Tian, H.; Yan, T.; Zhang, X.; Liu, S.; Sun, X.; Xu, L.; et al. One-Step Template-Free Fabrication of Ultrathin Mixed-Valence Polyoxovanadate-Incorporated Metal–Organic Framework Nanosheets for Highly Efficient Selective Oxidation Catalysis in Air. *ACS Appl. Mater. Interfaces* **2019**, *11*, 12786–12796. [[CrossRef](#)] [[PubMed](#)]
56. Hui, J.; Chu, H.; Zhang, W.; Shen, Y.; Chen, W.; Hu, Y.; Liu, W.; Gao, C.; Guo, S.; Xiao, G.; et al. Multicomponent metal–organic framework derivatives for optimizing the selective catalytic performance of styrene epoxidation reaction. *Nanoscale* **2018**, *10*, 8772–8778. [[CrossRef](#)] [[PubMed](#)]
57. Saedi, Z.; Safarifard, V.; Morsali, A. Dative and covalent-dative postsynthetic modification of a two-fold interpenetration pillared-layer MOF for heterogeneous catalysis: A comparison of catalytic activities and reusability. *Microporous Mesoporous Mater.* **2016**, *229*, 51–58. [[CrossRef](#)]
58. Berijani, K.; Morsali, A.; Hupp, J.T. An effective strategy for creating asymmetric MOFs for chirality induction: A chiral Zr-based MOF for enantioselective epoxidation. *Catal. Sci. Technol.* **2019**, *9*, 3388–3397. [[CrossRef](#)]
59. Noh, H.; Cui, Y.; Peters, A.W.; Pahls, D.; Ortuño, M.A.; Vermeulen, N.A.; Cramer, C.J.; Gagliardi, L.; Hupp, J.T.; Farha, O.K. An Exceptionally Stable Metal–Organic Framework Supported Molybdenum(VI) Oxide Catalyst for Cyclohexene Epoxidation. *J. Am. Chem. Soc.* **2016**, *138*, 14720–14726. [[CrossRef](#)]
60. Kardanpour, R.; Tangestaninejad, S.; Mirkhani, V.; Moghadam, M.; Mohammadpoor-Baltork, I.; Zadehahmadi, F. Efficient alkene epoxidation catalyzed by molybdenyl acetylacetonate supported on aminated UiO-66 metal–organic framework. *J. Solid State Chem.* **2015**, *226*, 262–272. [[CrossRef](#)]
61. Tang, J.; Dong, W.; Wang, G.; Yao, Y.; Cai, L.; Liu, Y.; Zhao, X.; Xu, J.; Tan, L. Efficient molybdenum(vi) modified Zr-MOF catalysts for epoxidation of olefins. *RSC Adv.* **2014**, *4*, 42977–42982. [[CrossRef](#)]
62. Liu, T.-F.; Vermeulen, N.A.; Howarth, A.J.; Li, P.; Sarjeant, A.A.; Hupp, J.T.; Farha, O.K. Adding to the Arsenal of Zirconium-Based Metal–Organic Frameworks: The Topology as a Platform for Solvent-Assisted Metal Incorporation. *Eur. J. Inorg. Chem.* **2016**, *27*, 4349. [[CrossRef](#)]
63. Pereira, C.; Biernacki, K.; Rebelo, S.L.; Magalhães, A.L.; Carvalho, A.P.; Pires, J.; Freire, C. Designing heterogeneous oxovanadium and copper acetylacetonate catalysts: Effect of covalent immobilisation in epoxidation and aziridination reactions. *J. Mol. Catal. A Chem.* **2009**, *312*, 53–64. [[CrossRef](#)]
64. Li, Z.; Wu, S.; Ding, H.; Lu, H.; Liu, J.; Huo, Q.; Guan, J.; Kan, Q. Oxovanadium(IV) and iron(III) salen complexes immobilized on amino-functionalized graphene oxide for the aerobic epoxidation of styrene. *New J. Chem.* **2013**, *37*, 4220–4229. [[CrossRef](#)]
65. Ben Zid, T.; Khedher, I.; Ghorbel, A. Chiral vanadyl salen catalyst immobilized on mesoporous silica as support for asymmetric oxidation of sulfides to sulfoxides. *React. Kinet. Mech. Catal.* **2010**, *100*, 131–143. [[CrossRef](#)]
66. Zamanifar, E.; Farzaneh, F. Immobilized vanadium amino acid Schiff base complex on Al-MCM-41 as catalyst for the epoxidation of allyl alcohols. *React. Kinet. Mech. Catal.* **2011**, *104*, 197–209. [[CrossRef](#)]
67. Pourkhosravani, M.; Dehghanpour, S.; Farzaneh, F.; Sohrabi, S. Designing new catalytic nanoreactors for the regioselective epoxidation of geraniol by the post-synthetic immobilization of oxovanadium(IV) complexes on a ZrIV-based metal–organic framework. *React. Kinet. Mech. Catal.* **2017**, *122*, 961–981. [[CrossRef](#)]
68. Tan, C.; Han, X.; Li, Z.; Liu, Y.; Cui, Y. Controlled Exchange of Achiral Linkers with Chiral Linkers in Zr-Based UiO-68 Metal–Organic Framework. *J. Am. Chem. Soc.* **2018**, *140*, 16229–16236. [[CrossRef](#)]
69. Huang, K.; Guo, L.L.; Wu, D.F. Synthesis of Metal Salen@MOFs and Their Catalytic Performance for Styrene Oxidation. *Ind. Eng. Chem. Res.* **2019**, *58*, 4744–4754. [[CrossRef](#)]
70. Xia, Q.; Li, Z.; Tan, C.; Liu, Y.; Gong, W.; Cui, Y. Multivariate Metal–Organic Frameworks as Multifunctional Heterogeneous Asymmetric Catalysts for Sequential Reactions. *J. Am. Chem. Soc.* **2017**, *139*, 8259–8266. [[CrossRef](#)]
71. Berijani, K.; Morsali, A. Construction of an Asymmetric Porphyrinic Zirconium Metal–Organic Framework through Ionic Postchiral Modification. *Inorg. Chem.* **2021**, *60*, 206–218. [[CrossRef](#)] [[PubMed](#)]
72. Martínez, H.; Cáceres, M.F.; Martínez, F.; Páez-Mozo, E.A.; Valange, S.; Castellanos, N.J.; Molina, D.; Barrault, J.; Arzoumanian, H. Photo-epoxidation of cyclohexene, cyclooctene and 1-octene with molecular oxygen catalyzed by dichloro dioxo-(4,4'-dicarboxylato-2,2'-bipyridine) molybdenum(VI) grafted on mesoporous TiO₂. *J. Mol. Catal. A Chem.* **2016**, *423*, 248–255. [[CrossRef](#)]

73. Portillo, A.S.; Navalón, S.; Cirujano, F.G.; I Xamena, F.X.L.; Alvaro, M.; Garcia, H. MIL-101 as Reusable Solid Catalyst for Autoxidation of Benzylic Hydrocarbons in the Absence of Additional Oxidizing Reagents. *ACS Catal.* **2015**, *5*, 3216–3224. [[CrossRef](#)]
74. Kou, J.; Sun, L.-B. Fabrication of Metal–Organic Frameworks inside Silica Nanopores with Significantly Enhanced Hydrostability and Catalytic Activity. *ACS Appl. Mater. Interfaces* **2018**, *10*, 12051–12059. [[CrossRef](#)] [[PubMed](#)]
75. Zhou, Z.; Li, X.; Wang, Y.; Luan, Y.; Li, X.; Du, X. Growth of Cu-BTC MOFs on dendrimer-like porous silica nanospheres for the catalytic aerobic epoxidation of olefins. *New J. Chem.* **2020**, *44*, 14350–14357. [[CrossRef](#)]
76. Zhao, J.; Wang, W.; Tang, H.; Ramella, D.; Luan, Y. Modification of Cu²⁺ into Zr-based metal–organic framework (MOF) with carboxylic units as an efficient heterogeneous catalyst for aerobic epoxidation of olefins. *Mol. Catal.* **2018**, *456*, 57–64. [[CrossRef](#)]
77. Wu, Y.; Wang, H.; Guo, S.; Zeng, Y.; Ding, M. MOFs-induced high-amphiphilicity in hierarchical 3D reduced graphene oxide-based hydrogel. *Appl. Surf. Sci.* **2021**, *540*, 148303. [[CrossRef](#)]
78. Canioni, R.; Roch-Marchal, C.; Sécheresse, F.; Horcajada, P.; Serre, C.; Hardi-Dan, M.; Férey, G.; Grenèche, J.-M.; Lefebvre, F.; Chang, J.-S.; et al. Stable polyoxometalate insertion within the mesoporous metal organic framework MIL-100(Fe). *J. Mater. Chem.* **2011**, *21*, 1226–1233. [[CrossRef](#)]
79. Wang, S.-S.; Yang, G.-Y. Recent Advances in Polyoxometalate-Catalyzed Reactions. *Chem. Rev.* **2015**, *115*, 4893–4962. [[CrossRef](#)]
80. Song, X.; Hu, D.; Yang, X.; Zhang, H.; Zhang, W.; Li, J.; Jia, M.; Yu, J. Polyoxomolybdenic Cobalt Encapsulated within Zr-Based Metal–Organic Frameworks as Efficient Heterogeneous Catalysts for Olefins Epoxidation. *ACS Sustain. Chem. Eng.* **2019**, *7*, 3624–3631. [[CrossRef](#)]
81. Villabrille, P.; Romanelli, G.; Gassa, L.; Vazquez, P.; Caceres, C. Synthesis and characterization of Fe- and Cu-doped molybdovanadophosphoric acids and their application in catalytic oxidation. *Appl. Catal. A Gen.* **2007**, *324*, 69–76. [[CrossRef](#)]
82. Jin, M.; Niu, Q.; Liu, G.; Lv, Z.; Si, C.; Guo, H. Encapsulation of ionic liquids into POMs-based metal–organic frameworks: Screening of POMs-ILs@MOF catalysts for efficient cycloolefins epoxidation. *J. Mater. Sci.* **2020**, *55*, 8199–8210. [[CrossRef](#)]
83. Ke, F.; Guo, F.; Yu, J.; Yang, Y.; He, Y.; Chang, L.; Wan, X. Highly Site-Selective Epoxidation of Polyene Catalyzed by Metal–Organic Frameworks Assisted by Polyoxometalate. *J. Inorg. Organomet. Polym. Mater.* **2017**, *27*, 843–849. [[CrossRef](#)]
84. Li, N.; Mu, B.; Lv, L.; Huang, R. Assembly of new polyoxometalate-templated metal–organic frameworks based on flexible ligands. *J. Solid State Chem.* **2015**, *226*, 88–93. [[CrossRef](#)]
85. Zhang, Y.; Li, Y.-X.; Liu, L.; Han, Z.-B. Palladium nanoparticles supported on UiO-66-NH₂ as heterogeneous catalyst for epoxidation of styrene. *Inorg. Chem. Commun.* **2019**, *100*, 51–55. [[CrossRef](#)]
86. Limvorapitux, R.; Chou, L.-Y.; Young, A.P.; Tsung, C.-K.; Nguyen, S.T. Coupling Molecular and Nanoparticle Catalysts on Single Metal–Organic Framework Microcrystals for the Tandem Reaction of H₂O₂ Generation and Selective Alkene Oxidation. *ACS Catal.* **2017**, *7*, 6691–6698. [[CrossRef](#)]
87. Jin, T.; Yang, Q.; Meng, C.; Xu, J.; Liu, H.; Hu, J.; Ling, H. Promoting desulfurization capacity and separation efficiency simultaneously by the novel magnetic Fe₃O₄@PAA@MOF-199. *RSC Adv.* **2014**, *4*, 41902–41909. [[CrossRef](#)]
88. Li, J.; Gao, H.; Tan, L.; Luan, Y.; Yang, M. Superparamagnetic Core-Shell Metal–Organic Framework Fe₃O₄/Cu₃(btc)₂Microspheres and Their Catalytic Activity in the Aerobic Oxidation of Alcohols and Olefins. *Eur. J. Inorg. Chem.* **2016**, *2016*, 4906–4912. [[CrossRef](#)]
89. Hou, J.; Luan, Y.; Yu, J.; Qi, Y.; Wang, G.; Lu, Y. Fabrication of hierarchical composite microspheres of copper-doped Fe₃O₄@P4VP@ZIF-8 and their application in aerobic oxidation. *New J. Chem.* **2016**, *40*, 10127–10135. [[CrossRef](#)]
90. Qi, Y.; Luan, Y.; Yu, J.; Peng, X.; Wang, G. Nanoscaled Copper Metal–Organic Framework (MOF) Based on Carboxylate Ligands as an Efficient Heterogeneous Catalyst for Aerobic Epoxidation of Olefins and Oxidation of Benzylic and Allylic Alcohols. *Chem. A Eur. J.* **2015**, *21*, 1589–1597. [[CrossRef](#)]
91. Yang, X.; Yuan, S.; Zou, L.; Drake, H.; Zhang, Y.; Qin, J.; Alsalmé, A.; Zhou, H.C. One-Step Synthesis of Hybrid Core–Shell Metal–Organic Frameworks. *Angew. Chem.* **2018**, *130*, 3991–3996. [[CrossRef](#)]
92. Aresta, M.; Dibenedetto, A.; Angelini, A. Catalysis for the Valorization of Exhaust Carbon: From CO₂ to Chemicals, Materials, and Fuels. Technological Use of CO₂. *Chem. Rev.* **2013**, *114*, 1709–1742. [[CrossRef](#)]
93. North, M.; Pasquale, R. Mechanism of Cyclic Carbonate Synthesis from Epoxides and CO₂. *Angew. Chem. Int. Ed.* **2009**, *48*, 2946–2948. [[CrossRef](#)]
94. Shi, L.; Xu, S.; Zhang, Q.; Liu, T.; Wei, B.; Zhao, Y.; Meng, L.; Li, J. Ionic Liquid/Quaternary Ammonium Salt Integrated Heterogeneous Catalytic System for the Efficient Coupling of Carbon Dioxide with Epoxides. *Ind. Eng. Chem. Res.* **2018**, *57*, 15319–15328. [[CrossRef](#)]
95. Shi, X.-L.; Chen, Y.; Duan, P.; Zhang, W.; Hu, Q. Conversion of CO₂ into Organic Carbonates over a Fiber-Supported Ionic Liquid Catalyst in Impellers of the Agitation System. *ACS Sustain. Chem. Eng.* **2018**, *6*, 7119–7127. [[CrossRef](#)]
96. Ziaee, M.A.; Tang, Y.; Zhong, H.; Tian, D.; Wang, R. Urea-Functionalized Imidazolium-Based Ionic Polymer for Chemical Conversion of CO₂ into Organic Carbonates. *ACS Sustain. Chem. Eng.* **2018**, *7*, 2380–2387. [[CrossRef](#)]
97. Yang, Z.; Yu, B.; Zhang, H.; Zhao, Y.; Chen, Y.; Ma, Z.; Ji, G.; Gao, X.; Han, B.; Liu, Z. Metalated Mesoporous Poly(triphenylphosphine) with Azo Functionality: Efficient Catalysts for CO₂ Conversion. *ACS Catal.* **2016**, *6*, 1268–1273. [[CrossRef](#)]
98. Sun, Q.; Aguila, B.; Perman, J.A.; Nguyen, N.T.-K.; Ma, S. Flexibility Matters: Cooperative Active Sites in Covalent Organic Framework and Threaded Ionic Polymer. *J. Am. Chem. Soc.* **2016**, *138*, 15790–15796. [[CrossRef](#)]

99. Beyzavi, M.H.; Stephenson, C.J.; Liu, Y.; Karagiari, O.; Hupp, J.T.; Farha, O.K. Metal-organic framework-based catalysts: Chemical fixation of CO₂ with epoxides leading to cyclic organic carbonates. *Front. Energy Res.* **2015**, *3*, 63. [[CrossRef](#)]
100. Bon, V.; Senkovskyy, V.; Senkovska, I.; Kaskel, S. Zr(IV) and Hf(IV) based metal-organic frameworks with reo-topology. *Chem. Commun.* **2012**, *48*, 8407–8409. [[CrossRef](#)]
101. Beyzavi, M.H.; Klet, R.C.; Tussupbayev, S.; Borycz, J.; Vermeulen, N.A.; Cramer, C.J.; Stoddart, J.F.; Hupp, J.T.; Farha, O.K. A Hafnium-Based Metal-Organic Framework as an Efficient and Multifunctional Catalyst for Facile CO₂ Fixation and Regioselective and Enantioselective Epoxide Activation. *J. Am. Chem. Soc.* **2014**, *136*, 15861–15864. [[CrossRef](#)]
102. Tran, Y.B.N.; Nguyen, P.T.K.; Luong, Q.T.; Nguyen, K.D. Series of M-MOF-184 (M = Mg, Co, Ni, Zn, Cu, Fe) Metal-Organic Frameworks for Catalysis Cycloaddition of CO₂. *Inorg. Chem.* **2020**, *59*, 16747–16759. [[CrossRef](#)]
103. Agarwal, R.A.; Gupta, A.K.; De, D. Flexible Zn-MOF Exhibiting Selective CO₂ Adsorption and Efficient Lewis Acidic Catalytic Activity. *Cryst. Growth Des.* **2019**, *19*, 2010–2018. [[CrossRef](#)]
104. Hayashi, H.; Côté, A.P.; Furukawa, H.; O’Keeffe, M.; Yaghi, O.M. Zeolite A imidazolate frameworks. *Nat. Mater.* **2007**, *6*, 501–507. [[CrossRef](#)] [[PubMed](#)]
105. Huang, A.; Chen, Y.; Wang, N.; Hu, Z.; Jiang, J.; Caro, J. A highly permeable and selective zeolitic imidazolate framework ZIF-95 membrane for H₂/CO₂ separation. *Chem. Commun.* **2012**, *48*, 10981–10983. [[CrossRef](#)] [[PubMed](#)]
106. Bhin, K.M.; Tharun, J.; Roshan, K.R.; Kim, D.-W.; Chung, Y.; Park, D.-W. Catalytic performance of zeolitic imidazolate framework ZIF-95 for the solventless synthesis of cyclic carbonates from CO₂ and epoxides. *J. CO₂ Util.* **2017**, *17*, 112–118. [[CrossRef](#)]
107. Liang, J.; Chen, R.-P.; Wang, X.-Y.; Liu, T.-T.; Wang, X.-S.; Huang, Y.-B.; Cao, R. Postsynthetic ionization of an imidazole-containing metal-organic framework for the cycloaddition of carbon dioxide and epoxides. *Chem. Sci.* **2017**, *8*, 1570–1575. [[CrossRef](#)] [[PubMed](#)]
108. Ding, L.-G.; Yao, B.-J.; Jiang, W.-L.; Li, J.-T.; Fu, Q.-J.; Li, Y.-A.; Liu, Z.-H.; Ma, J.-P.; Dong, Y.-B. Bifunctional Imidazolium-Based Ionic Liquid Decorated UiO-67 Type MOF for Selective CO₂ Adsorption and Catalytic Property for CO₂ Cycloaddition with Epoxides. *Inorg. Chem.* **2017**, *56*, 2337–2344. [[CrossRef](#)]
109. Kurisingal, J.F.; Rachuri, Y.; Pillai, R.S.; Gu, Y.; Choe, Y.; Park, D. Ionic-Liquid-Functionalized UiO-66 Framework: An Experimental and Theoretical Study on the Cycloaddition of CO₂ and Epoxides. *ChemSusChem* **2019**, *12*, 1033–1042. [[CrossRef](#)]
110. Ding, M.; Jiang, H.-L. Incorporation of Imidazolium-Based Poly(ionic liquid)s into a Metal-Organic Framework for CO₂ Capture and Conversion. *ACS Catal.* **2018**, *8*, 3194–3201. [[CrossRef](#)]
111. Pander, M.; Janeta, M.; Bury, W. Quest for an Efficient 2-in-1 MOF-Based Catalytic System for Cycloaddition of CO₂ to Epoxides under Mild Conditions. *ACS Appl. Mater. Interfaces* **2021**, *13*, 8344–8352. [[CrossRef](#)] [[PubMed](#)]
112. Zhu, J.; Usov, P.M.; Xu, W.; Celis-Salazar, P.J.; Lin, S.; Kessinger, M.C.; Landaverde-Alvarado, C.; Cai, M.; May, A.M.; Slobodnick, C.; et al. A New Class of Metal-Cyclam-Based Zirconium Metal-Organic Frameworks for CO₂ Adsorption and Chemical Fixation. *J. Am. Chem. Soc.* **2018**, *140*, 993–1003. [[CrossRef](#)] [[PubMed](#)]
113. Vitillo, J.G.; Savonnet, M.; Ricchiardi, G.; Bordiga, S. Tailoring Metal-Organic Frameworks for CO₂ Capture: The Amino Effect. *ChemSusChem* **2011**, *4*, 1281–1290. [[CrossRef](#)] [[PubMed](#)]
114. Torrisi, A.; Bell, R.G.; Mellot-Draznieks, C. Functionalized MOFs for Enhanced CO₂ Capture. *Cryst. Growth Des.* **2010**, *10*, 2839–2841. [[CrossRef](#)]
115. Senthilkumar, S.; Maru, M.S.; Somani, R.S.; Bajaj, H.C.; Neogi, S. Unprecedented NH₂-MIL-101(Al)/n-Bu₄NBr system as solvent-free heterogeneous catalyst for efficient synthesis of cyclic carbonates via CO₂ cycloaddition. *Dalton Trans.* **2018**, *47*, 418–428. [[CrossRef](#)]
116. Zhu, M.; Carreon, M.A. Porous crystals as active catalysts for the synthesis of cyclic carbonates. *J. Appl. Polym. Sci.* **2014**, *131*. [[CrossRef](#)]
117. Cai, T.; Liu, J.; Cao, H.; Cui, C. Synthesis of bio-based cyclic carbonate from vegetable oil methyl ester by CO₂ fixation with acid-base pair MOFs. *Ind. Crop. Prod.* **2020**, *145*, 112155. [[CrossRef](#)]
118. Mercuri, G.; Moroni, M.; Domasevitch, K.V.; Di Nicola, C.; Campitelli, P.; Pettinari, C.; Giambastiani, G.; Galli, S.; Rossin, A. Carbon Dioxide Capture and Utilization with Isomeric Forms of Bis(amino)-Tagged Zinc Bipyrazolate Metal-Organic Frameworks. *Chem. A Eur. J.* **2021**, *27*, 4746–4754. [[CrossRef](#)]
119. Norouzi, F.; Khavasi, H.R. Diversity-Oriented Metal Decoration on UiO-Type Metal-Organic Frameworks: An Efficient Approach to Increase CO₂ Uptake and Catalytic Conversion to Cyclic Carbonates. *ACS Omega* **2019**, *4*, 19037–19045. [[CrossRef](#)]
120. Li, J.; Ren, Y.; Yue, C.; Fan, Y.; Qi, C.; Jiang, H. Highly Stable Chiral Zirconium-Metallosalen Frameworks for CO₂ Conversion and Asymmetric C–H Azidation. *ACS Appl. Mater. Interfaces* **2018**, *10*, 36047–36057. [[CrossRef](#)]